Author/s:
Priscilla, N;Sulejman, SB;Roberts, A;Wesemann, L

Title:
New Avenues for Phase Imaging: Optical Metasurfaces

Date:
2024-08-21

Citation:
Priscilla, N., Sulejman, S. B., Roberts, A. & Wesemann, L. (2024). New Avenues for Phase Imaging: Optical Metasurfaces. ACS Photonics, 11 (8), pp.2843-2859. https://doi.org/10.1021/acsphotonics.4c00359.

Persistent Link:
https://hdl.handle.net/11343/354835

New avenues for phase imaging: optical metasurfaces

Niken Priscilla,[†,‡] Shaban B. Sulejman,[†,‡] Ann Roberts,[†] and Lukas Wesemann[*,†]

†*ARC Centre of Excellence for Transformative Meta-Optical Systems, School of Physics, The University of Melbourne, VIC 3010, Australia*

‡*These authors have contributed equally and share first authorship*

E-mail: lukas.wesemann@unimelb.edu.au

Abstract

Visualizing the phase of an optical field is fundamental to applications ranging from biological microscopy through to material science. Its importance is evidenced by the award of the 1953 Nobel Prize to Frits Zernike for his invention of the phase contrast microscope. Conventional phase imaging techniques, including Zernike phase contrast, differential interference contrast and interferometry, often rely on bulky optical components and macroscopic propagation distances. These factors hinder the miniaturization and integration into ultra-compact imaging systems. Furthermore, computational methods also present challenges due to computational complexity, potentially compromising speed and energy efficiency. The recent emergence of the use of nano-optics, including thin films and metasurfaces, in image processing has opened up possibilities for a new class of compact methods for phase imaging. These nano-structured devices have been shown to permit phase visualization and we believe that they hold the potential to enable the next generation of imaging systems and photo-detectors in a broad range of applications.

Keywords

Phase imaging, meta-optics, metasurfaces, microscopy, imaging, wavefront sensing

1 Introduction

The use of meta-optics in imaging systems has attracted significant attention from the scientific community in recent years.[1] These nano-photonic devices hold the promise of reducing the spatial footprint of the key components in conventional imaging systems and enabling unprecedented functionality.[2] Some examples of successful demonstrations of meta-optical devices relevant to imaging systems include flat lenses,[3] polarizers,[4,5] wave-plates,[6] beam-splitters[7–10] and multi-functional components.[11] These underpin our opinion that meta-optics will play a pivotal role in the ongoing transition to compact imaging systems. Meta-optical devices have also been demonstrated to permit processing of images to modify them, or extract information from a wavefield.[12] Most of the initial work in this field has focused on devices that perform high-pass spatial frequency filtering to perform spatial differentiation and edge detection on amplitude image. Other devices have been demonstrated to perform mathematical operations such as differentiation,[13,14] Fourier transformation,[15,16] or solving integral equations.[17]

More recently, meta-optical devices have gained attention as new methods to extract and visualize the phase of an optical field.[18–21] For a scalar electric field U with

$$U(x, y) = A(x, y) \exp[i\varphi(x, y)], \tag{1}$$

where $A(x, y)$ describes the field amplitude and $\varphi(x, y)$ refers to its phase in a fixed plane on the optical (z) axis, the intensity or irradiance I is given by

$$I(x, y) \propto |U(x, y)|^2 = A(x, y)^2. \tag{2}$$

The intensity distribution can be sensed using conventional photo-detector technology. The phase $\varphi(x, y)$, however, remains invisible and alternative methods are required to visualize it.

Visualizing the phase of an optical field is a fundamental enabler for biomedical research. In particular, the study of biological cells heavily relies on it and has historically driven the development of phase imaging methods. Imaging contrast in transparent biological specimens can also be enhanced through the introduction of exogenous staining agents. However, this often requires fixing the samples and therefore prevents long-term studies via live-cell imaging. For some types of cells, like mammalian stem cells, biological compatibility with staining agents is particularly challenging.[22] Phase imaging enables visualising refractive index and thickness variations within transparent samples without the need for staining. Furthermore, extracting quantitative phase maps from an optical field is also critical to wavefront recovery required for adaptive optics systems, and determining the direction of propagation of light in free space.

In this perspective, we contrast conventional techniques for visualizing and quantifying the phase of light with emerging meta-optical approaches. We believe that the latter have the potential to address some of the limitations of conventional phase imaging technology, including cost, spatial footprint and processing times of computational methods. Furthermore, we anticipate that meta-optics will be an enabling technology for the next generation of compact phase imaging and wavefront sensing systems with capabilities beyond those of state of the art approaches. The interested reader is referred to more general articles on image processing and analog computing, including Wesemann *et al.*[12] or Zangeneh-Nejad *et al.*,[23] for a broader discussion of further applications of meta-optics in image manipulation.

2 Conventional phase imaging methods

As light propagates through transparent samples, it accumulates a spatially varying phase shift arising from variations in their refractive index or other interactions. These modulations are invisible to conventional bright field microscopes, which has driven the development of a variety of phase imaging techniques.

2.1 Qualitative phase imaging

The conceptual groundwork for phase imaging was laid in the mid-1930s by Frits Zernike, who introduced a new technique for visualizing unstained transparent samples.[24–26] The core component of the phase microscope was a phase plate positioned in the back focal plane of a microscope objective. It introduces a phase difference of $\pi/2$ between the light that has transmitted through the sample and the unmodified background light. The subsequent interference between these beams in the image plane of the sample generates contrast in the output image. In recent developments, the concept of Zernike phase plate has been extended to a spiral phase plate that creates a vortex in the wavefront of light, useful for spiral phase contrast microscopy[27,28] and Hilbert microscopy.[29,30] However, the images produced by phase contrast microscopes employing the use of phase plates can be limited by the presence of halo artifacts around the edges of objects.

In the early 1950s, Georges Nomarski developed a new type of phase contrast microscopy that avoided the need for Fourier-based filtering. The technique, known as differential interference contrast (DIC) microscopy,[31,32] involves the shearing of polarized light into two slightly displaced and orthogonally polarized beams with a Wollaston prism. The beams accumulate different phase shifts as they traverse slightly spatially separated paths through the sample and hence interfere when they are recombined. As a result, contrast is created in the output image producing a characteristic three-dimensional effect due to the relative optical path length differences along the shear direction. The technique forms part of a

broader category of phase gradient microscopy techniques that convert the gradual changes in the refractive index or thickness in transparent samples into intensity.[33,34] Phase gradient microscopy can also be used alongside computational techniques for quantitative phase imaging, such as by integrating the measured derivatives through Fourier-based integration. However, shear artifacts can appear in the images due to the shearing of polarized light and its interaction with birefringent samples.

Modulation contrast microscopy[35,36] relies on the use of a Hoffman modulator that exhibits a variable amplitude transmittance to enhance the visibility of phase variations in a transparent sample. This addressed some of the limitations associated with Zernike and Nomarski microscopy, such as reduced contrast or the appearance of artifacts in images where the phase variations are too strong. However, the system has a strong sensitivity to the phase only along a particular direction and therefore requires specific positioning of the sample. Other techniques have been developed, such as dark field microscopy that blocks directly transmitted light to generate images with stark contrast against a dark background.[37,38] While useful for imaging the larger features in a sample, dark field microscopy tends to yield weaker contrast for weakly scattering samples. Schlieren imaging is a Fourier-based method where either negative or positive spatial frequencies in the sample are removed by an optical 'knife edge',[39,40] but it requires the precise positioning of the knife in the Fourier transform plane of the sample.

Nanoparticles[41] and surface plasmon resonances,[42,43] originally used for enhancing contrast, have also been applied to phase contrast imaging. The latter technique leverages resonances that are highly sensitive to the refractive index of the surrounding material, providing a powerful tool for studying molecular interactions and drug screening processes. Balaur *et al.*[44] also demonstrated the conversion of small, local variations in refractive index into contrast using a nanopatterned silver film in the near-field vicinity of human tissue samples. Single-pixel imaging[45,46] has gained attention for its ability to access wavelengths beyond the capabilities of regular cameras, but is still currently limited by low resolution in

images. Finally, quantum mechanical effects[47,48] and defocusing techniques[49,50] have been employed to provide a variety of solutions to address the challenges associated with visualizing transparent samples. However, as we will discuss in detail in section 3, metasurfaces are presenting as effective solutions to many of the limitations associated with phase contrast microscopy techniques by removing the need for Fourier-based components, tailoring and tuning optical shearing, as well as extending the performance to wavelengths beyond the visible and near-infrared.

2.2 Quantitative phase imaging

Phase contrast imaging provides visual insight into the morphology and composition of transparent samples, which can be crucial in cancer imaging[51] and real-time blood testing.[52] However, the qualitative nature of this imaging method does not provide quantitative information of the phase variations in optical fields. Developments in quantitative phase imaging have opened opportunities to address this limitation. The Shack-Hartmann wavefront sensor is widely used for quantitative phase measurements, achieved by integrating the local phase slopes from microlenses that divert light onto a camera.[53] These devices are commercially available and are compatible with many conventional microscope systems, however the number of microlenses constrain the spatial resolution of the system.

Since the invention of the laser, a well-known method for acquiring relative phase information within optical fields is interferometry.[54–56] In this technique, coherent light that is transmitted through a transparent sample is combined with a reference beam to create an interferogram, which has an intensity that is a function of the phase difference between the two beams. Variations of the technique include shearing interferometry,[57,58] optical quadrature microscopy,[59] spatial[60–62] and gradient light interference microscopy,[63,64] phase-shifting interferometry[65,66] and differential phase contrast microscopy.[67–69]

A closely related technique is holographic microscopy.[70,71] This approach can capture both amplitude and phase information from a sample by recording its hologram. A quanti-

tative phase image can then be reconstructed computationally from the fringe pattern obtained via phase unwrapping algorithms. Digital holography has further diversified into other techniques including off-axis digital holography[72,73] and diffractive phase microscopy.[52,74]

Interferometry and holography are distinguished by their ability to deliver precise measurements of the relative phase shifts with high signal-to-noise ratios. However, they often feature relatively complex and sensitive configurations that require coherent illumination and stable environmental conditions, although, recent developments have allowed for partial coherence, such as in scanning white light interferometry.[75,76] Interferometric systems can also be limited by quadrature phase shift errors that introduce aberrations into the images. Metasurfaces can address these issues by removing the need for reference beams and reduce the overall size of the system. Speckle patterns, a common by-product of coherent illumination, have also been harnessed as a basis for quantitative phase imaging techniques.[77,78] By determining the optical path length differences across a sample, these methods can produce comprehensive maps detailing the thickness, refractive index or density of the sample. Depth information is also accessible in holography, enabling three-dimensional reconstructions that can be faster than other techniques such as optical coherence tomography[79,80] or optical diffraction tomography.[81–83]

2.3 Computational phase imaging

With the emergence of digital technology, computational approaches to phase imaging that rely on the algorithmic analysis of intensity measurements have gained prominence.[84] Early phase retrieval methods include the Gerchberg-Saxton algorithm[85] and the Fienup hybrid input-output algorithm.[86] There also exist methods that solve differential equations to retrieve the phase distribution of a transparent sample, including the Fokker-Planck equation[87,88] and the transport of intensity equation.[89–91] The latter encapsulates the manifestation of phase information in intensity variations as a result of the propagation of light and

is given in the paraxial approximation by

$$-k\frac{\partial I(x,y,z)}{\partial z} = \nabla_\perp \cdot \left(I(x,y,z)\nabla_\perp \varphi(x,y) \right) , \tag{3}$$

where $\nabla_\perp$ is the transverse (x, y) gradient operator and $k = 2\pi/\lambda$ is the wave-number and λ is the wavelength. The phase distribution $\varphi(x, y)$ can be solved by obtaining the intensity in two closely spaced planes along the optical (z) axis. These computational techniques shift the focus from optical manipulation to digital power, eliminating the need for external reference beams, phase-sensitive components or strict coherence requirements. However, the need to capture the intensity in two different planes requires mechanical shifts in the imaging system or additional optical complexity. Metasurfaces are bypassing this, however, by simultaneously producing the images required for image reconstruction.[92] However, the resulting images can be susceptible to the appearance of low frequency artifacts.

A prominent hybrid quantitative phase imaging technique that can surpass the diffraction limit is ptychography.[93] In this method, the sample is sequentially illuminated point-by-point to produce diffraction patterns that are combined in an iterative algorithm, such as the ptychographic iterative engine,[94] to recover the phase image. Fourier ptychography is a common variation of this technique, where the sample is illuminated with angled plane waves that select the spatial frequency components of a sample, which can be recombined with the Fourier transform.[95] A significant advantage of ptychography is the ability to simultaneously reconstruct the amplitude and phase of the complex wave, which reduces artifacts and improves the resolution. Metasurfaces are also being used to enhance the reconstructed amplitude and phase,[96] however the point-by-point scanning nature of ptychography can be relatively long. Additionally, the use of near-field effects may lead to additional complexity in retrieving the phase quantitatively, as the refractive index of the sample can be altered in the proximity of the device used. Artificial intelligence and machine learning have recently been advanced to offer a powerful addition to hybrid phase imaging systems.[97,98] These advanced systems

can analyze the output images to identify specific biological, pathological or other pertinent features,[99] which can be instrumental in detecting early stage cancer or diseases.[44,100]

3 Metasurface-enabled phase imaging methods

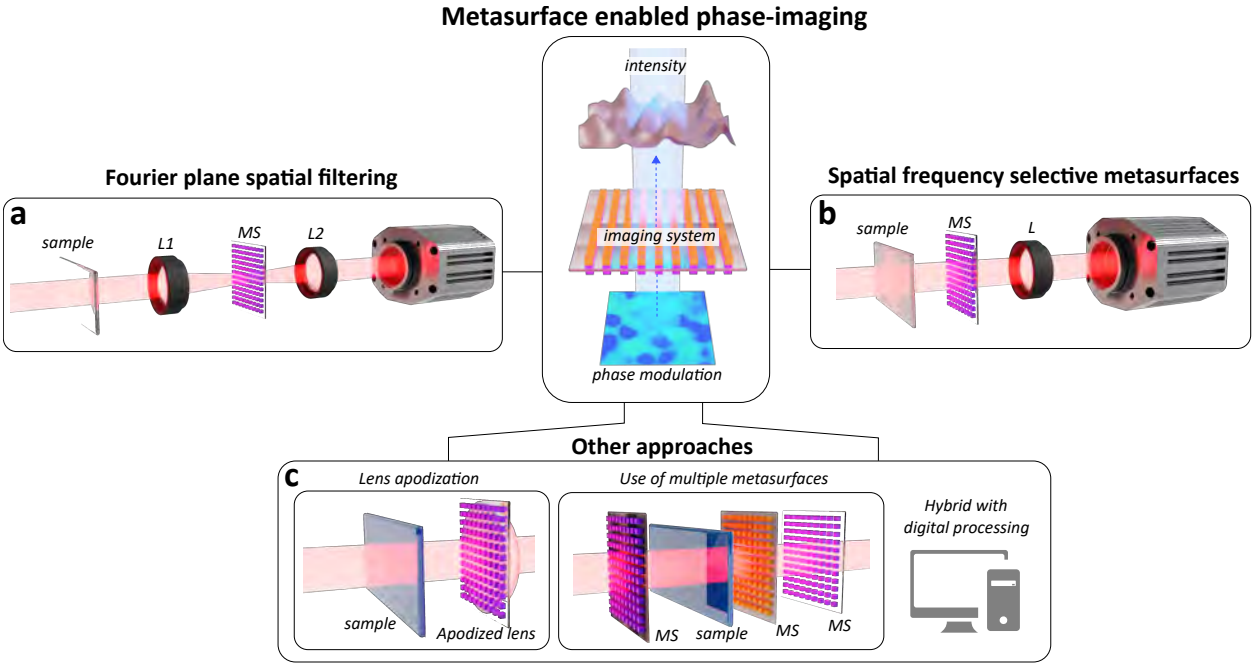

Figure 1: Techniques for meta-optical phase imaging. (a) Metasurface spatial-filters for placement in the Fourier plane of a $4f$-system. (b) Spatial frequency selective metasurfaces for filtering in the object- or image plane, sometimes refereed to as Green's function approach. (c) Other methods including metasurface-enabled lens apodization, the use of multiple metasurfaces and quantitative phase imaging via hybrid approaches involved metasurfaces and digital computation. 'L' stands for lens and 'MS' for metasurface.

While qualitative and quantitative methods for phase imaging are widely used, their implementation usually requires bulky, complex, and/or expensive components or computationally intensive algorithms. Meta-optical devices have gained significant attention as an enabling technology for miniaturizing imaging systems, including for novel approaches to phase imaging. Metasurfaces, in particular, enable complex light-matter interactions through the use of nano-structures[101] and this section reviews the use of meta-optical devices for phase contrast imaging applications.

The key advantages offered by metasurface phase imaging approaches are the unique combination of the flat nature of metasurfaces, the inherent flexibility in the design of optical metasurfaces, and in many cases their ability to process images in real-time without additional computational processing. This opens up new avenues for phase imaging systems not achievable with conventional methods. These include metasurfaces integrated with photodetectors[102] to extend their sensing capabilities from intensity to phase, as well as phase imaging systems directly integrated into microfluidic systems.[103,104] An additional promising avenue are ultra-compact wavefront sensing systems for applications with challenging requirements on data rates, form factor and energy consumption such as in small scale satellite systems,[105] where adaptive optics are commonly applied for wavefront correction.[106]

As indicated in the introduction to this perspective, biological imaging represents one of the key application areas of phase imaging. In particular live-cell phase imaging and quantitative phase imaging could benefit from metasurface based methods. Many of the qualitative phase-imaging approaches reviewed in this section are all-optical and thus inherently operate in real-time thus imposing no limit on time resolution. For those approaches that enable quantitative phase imaging via metasurfaces, computational post processing is involved and the time resolution depends on the execution speed of the post processing step.

The various metasurface enabled approaches can be divided into three different categories based on the role of the meta-optic within the imaging system. The first category implements meta-optical devices as spatial filters that are placed in the Fourier plane of a $4f$, or similar, system to manipulate optical fields in a way that visualizes the phase. The second category encompasses approaches that filter the spatial frequency spectrum of an optical field directly in the object or image plane. The third category combines several aspects from the first two categories and can integrate multiple meta-optical devices or devices with multiple functionalities.

3.1 Fourier plane spatial filtering using local metasurfaces

The first demonstrations of image processing were performed in the 1940s taking advantage of the well-known Fourier transforming property of a lens.[107–109] This involved the use of optical assemblies such as the $4f$ system where two lenses are used to access the Fourier plane of an incident wavefield where masks with a spatially varying amplitude and/or phase transmission are introduced to modify the spatial frequency content of the input field. Most significantly, both the amplitude and phase of the field can be accessed and modified using this technique. In the context of phase imaging, as discussed above, phase masks such as those used in Zernike phase contrast microscopy can be used to introduce a $\pi/2$ phase difference between the background (manifesting as zero spatial frequency) and the remainder of the field. Furthermore, all-optical systems are effectively real-time and require no further energy input other than the incident field. Ultimately, the quality of the processed image will depend on the spatial resolution of the mask which will determine the precision with which individual spatial frequency components can be addressed, and the transverse size of the mask and numerical aperture of the entire imaging system. The extent to which the amplitude and phase of the light transmitted through the mask can be independently controlled are also significant. Note that spatial filters can be introduced in both transmission and reflection systems where, in the latter, the same lens Fourier and inverse Fourier transforms the field.[110]

In terms of progressing Fourier plane spatial frequency filtering, meta-optics provides a number of opportunities (Fig. 1a). Firstly, with the capacity for independent control of the amplitude and phase of transmission through a metasurface[114] they provide a new paradigm for developing meta-optic spatial filters. Secondly, metalenses can reduce the overall size dedicated to optical components in a $4f$ or other system and, finally, the new concept of space plates[115] may reduce the physical dimensions of the required propagation distances.

Spatial filters based on nanostructures can be realized by introducing into the transmitted, or less frequently the reflected, field a point-by-point variation in amplitude and/or

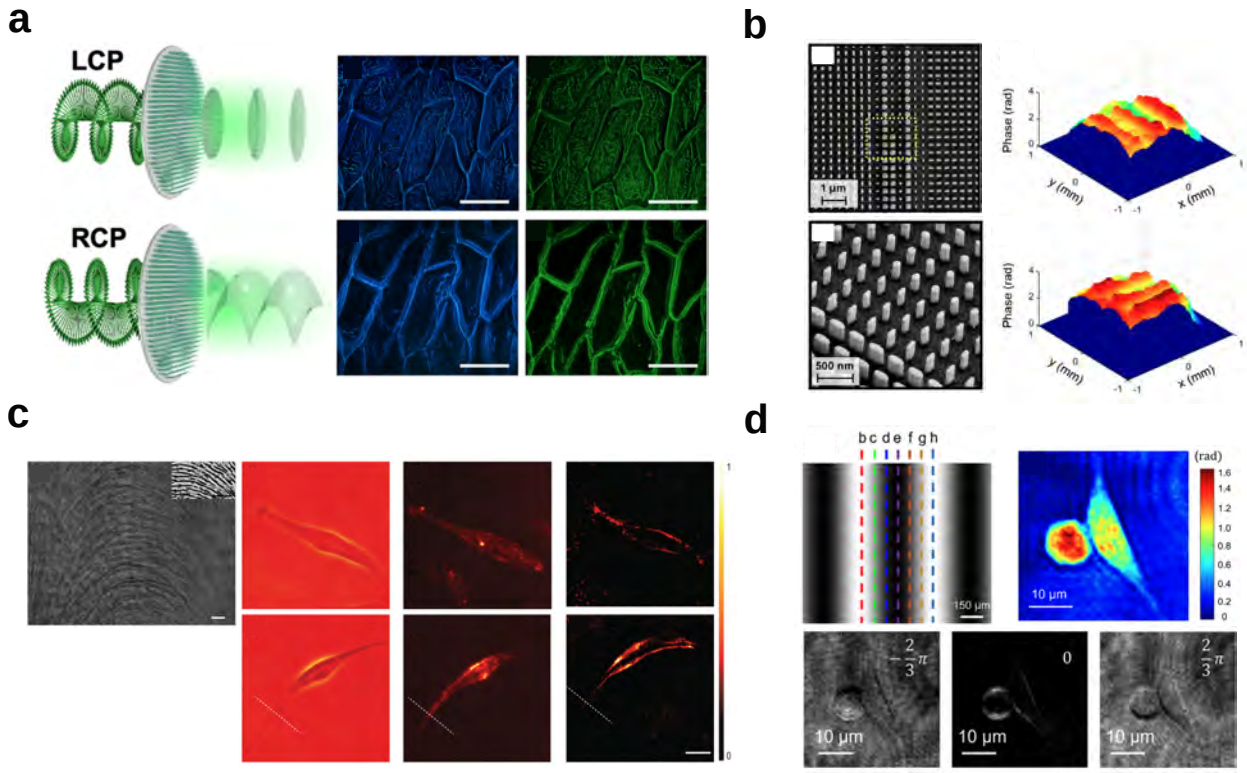

Figure 2: Phase imaging in the Fourier plane using local metasurfaces. **a)** Dielectric metasurface enabling bright field imaging and edge detection switchable via the handedness of circularly polarised light (left), imaging of undyed onion epidermal cells (right). Adapted with permission from ref.[111] Copyright 2020 American Chemical Society. **b)** SEM image of metasurface spatial filter in top-view and tilted view (left) and quantitative phase map obtained via metasurface assisted transport of intensity (TIE) imaging (right). Adapted with permission from ref.[92] Copyright 2021 American Chemical Society. **c)** Polariscope image of femtosecond laser engraved spatial filter (left), obtained images using the metasurfaces (right) of humanumbilical vein endothelial cell (HUVEC) (top row) and human bronchial epithelial cell (HBEC) (bottom row). Shown are phase contrast (first column), darkfield imaging (second column) and edge detection (third column).[112] Copyright 2020 Author(s), licensed under a Creative Commons Attribution (CC BY 4.0) license. **d)** Fourier optical spin splitting microscopy - transmittance of metasurface spatial filter (top left), qualitative (bottom) and quantitative (top right) phase imaging of NIH3T3 cells. Reprinted figure with permission from ref.[113] Copyright 2022 by the American Physical Society.

phase via a mask placed in the Fourier transform plane. One mechanism to do this is utilizing the concept of the geometric or Pancharatnam-Berry (PB) phase[116–118] to engineer local phase variations across a metasurface. Through the use of tailored dielectric or plasmonic 'nanoblocks' or 'nanoslots' a, full 2π phase coverage can be achieved to create complex phase masks when illuminated with circularly polarized light.[1,119] The use of non-resonant structures can result in broadband performance.[112]

As discussed earlier, the use of a spiral phase plate as a spatial filter leads to isotropic edge enhancement in the resulting image, regardless of the orientation of the object. For example, Huo *et al.*[111] leveraged the concept of geometric phase by performing spin multiplexing with TiO_2 nanopillars (Fig. 2a). Upon LCP illumination, bright field amplitude imaging of phase objects can be observed, while edge-enhanced phase contrast is shown with RCP illumination. This configuration was used to demonstrate phase-contrast imaging of onion epidermal cells at wavelengths from 480-630 nm, showcasing its broadband functionality. Another demonstration by Xu *et al.*[120] utilized an inverse design approach based on the evolution of the Pancharatnam–Berry (PB) phase on the Poincaré sphere. This method enables the design of various metasurfaces with different optical transfer functions, including those tailored for phase imaging applications.

Shou *et al.*[121] demonstrated second-order differentiation with respect to two orthogonal directions by cascading two $4f$ systems where dielectric PB phase metasurfaces are used as orthogonally oriented spatial filters in the two Fourier planes. Similarly, Wang *et al.*[122] used identical metasurfaces oriented in orthogonal directions in an interferometric setup. One metasurface, placed in one arm of the interferometer, performs spatial differentiation along the x-direction, while the other along the y-direction. On interference, the two processes achieve isotropic edge-enhanced phase contrast images.

Phase edge enhancement through spatial differentiation in a $4f$ setup can be performed using a birefringent PB metasurface produced using femtosecond pulse laser processing of silica[112,123] (Fig. 2c). Broadband phase edge enhanced images of human umbilical vein

endothelial cells and human brain endothelial cells were demonstrated.

Zhou *et al.*[113] used a PB phase dielectric metasurface in conjunction with crossed linear polarizers to create a spatial filter with a sinusoidally varying transmittance in the Fourier plane (Fig. 2d) taking advantage of the difference in phase introduced into the RCP and LCP components of the transmitted field. Mechanically displacing the metasurface or rotating the analyzer introduces a phase bias between the resulting copies of the phase contrast images permitting computational quantification of the phase. The authors performed single-shot QPI on NIH3T3 cells by combining this process with a polarization-sensitive camera.

Phase variations can also be visualized by introducing resonant nanostructures[124] and taking advantage of Mie or other resonances in the scatterers, although there have been fewer demonstrations of using this approach to performing phase imaging. One example[125] uses a device composed of polycrystalline silicon (P-Si) nanoblocks of different sizes on a glass substrate to obtain a 2π phase variation across the surface. Edge detection of rhizobia (soybean roots) and liver tissue was demonstrated using linearly polarised illumination at 830 nm. Unlike the PB approach, the use of resonant nanostructures leads to a limited bandwidth although usually requiring less complex polarization strategies. Metasurfaces can also play a crucial role in providing information for both the TIE and other phase retrieval processes. Engay *et al.*[92] utilize a resonant metasurface in the Fourier plane that separates linearly polarized light into two orthogonal polarization components (TE and TM) and introducing a propagation phase shift onto the TM component removing the requirement for the mechanical defocus typically required for applying the TIE (Fig. 2b) and enabling single-shot image acquisition.

3.2 Spatial-frequency selective metasurfaces in the object or image plane

Despite its benefits, a $4f$ system is relatively bulky requiring not only lenses, but also the propagation distances required for the optical field to evolve to the Fourier plane and back.

Secondly, the mask needs to be placed in the Fourier plane with errors in axial and transverse positioning leading to loss of quality of the processed image. Metasurfaces with a sensitivity to the angle of incidence, on the other hand, are capable of performing image processing where the incident angles, associated with the various plane wave components in a decomposition, correspond to specific spatial frequencies (Fig. 1b). Unlike Fourier plane spatial filtering discussed in the previous section, the additional optics associated with a $4f$ system are not required and, furthermore, there is considerable flexibility in positioning the metasurface in the optical system. For example, a suitably designed metasurface could be placed in proximity to the object of interest, in the object plane, adjacent to a lens, or at some other location minimizing the overall size of the optical system.

For monochromatic, coherent light propagating through a linear optical system, the input field can be decomposed into a superposition of plane waves with their (complex) amplitudes connected to the incident field via Fourier transformation. Taking the $z-$ direction to be the optical axis, the relationship between the transverse components of the spatial frequency (k_x, k_y) and the angles of propagation of the associated plane wave (θ, ϕ) is given by:

$$k_x = k_0 \sin\theta \cos\phi \tag{4}$$

$$k_y = k_0 \sin\theta \sin\phi \tag{5}$$

where $k_0 = 2\pi/\lambda$ for light with free-space wavelength λ, θ denotes the polar angle with respect to the optical axis and ϕ the angle of the projection of the wavevector onto the $x-y$ plane with respect to the x-axis. It is, therefore, apparent that metasurfaces and other nanophotonic devices with a transmission or reflection that is sensitive to the angle of incidence can be used for image manipulation, more generally, and phase imaging, in particular. We here refer to this method as the 'object plane' approach and the interaction of the device with an incident optical field is most appropriately described in terms of an optical transfer function (OTF) $H(k_x, k_y)$. In the not uncommon case of a device that

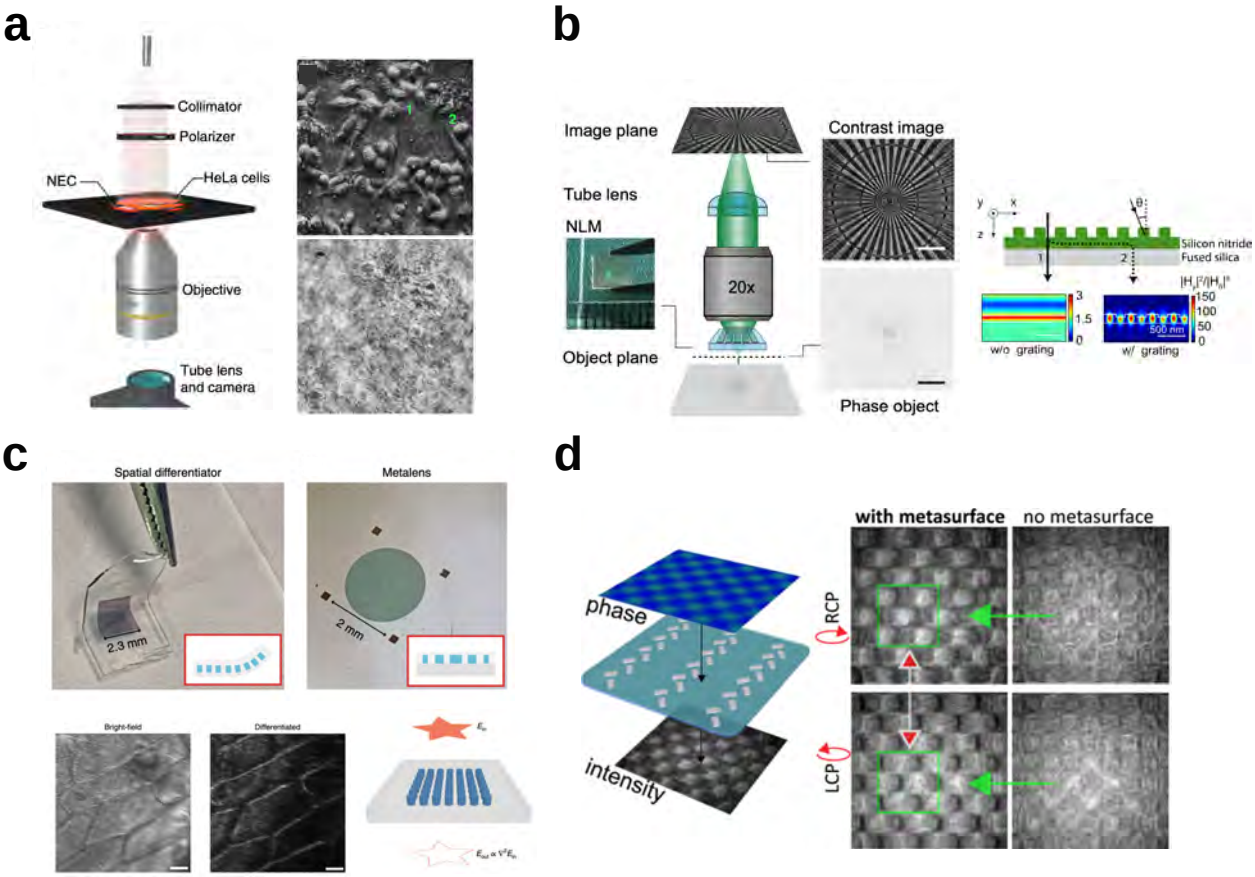

Figure 3: Phase imaging using spatial frequency selective meta-optics. **a)** Nanophotonics enhanced coverslip (NEC) based on Ag/TiO_2 resonant waveguide gratings enabling phase visualisation. The phase object is directly placed on top of the NEC (left). Pseudo-3D images, similar to DIC images, are generated of human cervical cancer cells (HeLa) (top right) with brightfield image for reference (bottom right).[19] Copyright 2021 Author(s), licensed under a Creative Commons Attribution (CC BY-NC-ND 4.0) license. **b)** Quantitative phase imaging in transmission (left) using Silicon Nitride resonant waveguide gratings (right). Phase objects are directly placed in front of the metasurface filter.[20] Copyright 2022 Author(s), licensed under a Creative Commons Attribution (CC BY-NC-ND 4.0) license. **c)** Photonic crystal device for high-pass spatial frequency filtering in transmission (bottom right), and integration with metalens (top). Demonstration of edge detection in images of onion epidermis using the compound device. Adapted from ref.[18] with permission from Springer Nature. **d)** Metasurface with asymmetric angular response based on 'spin-orbit coupling' of incident circularly polarised light. DIC-like images of phase object are generated without requirement for off-normal illumination. Adapted with permission from ref.[21] Copyright 2022 American Chemical Society.

possesses a polarization sensitivity, this function is replaced by a tensor that describes the transmission of the polarization basis states through the structure. In this case, the OTF is generally one of the co- or cross-polarized components of transmission or reflection. The object plane approach can also be used to perform mathematical operations on an incident field. For example, if the OTF is proportional to the x-component of the incident wavevector, i.e., $H(k_x, k_y) \propto k_x$, the resulting output is the derivative with respect to x of the input. First and second order differentiation also provide an avenue to edge detection of an input amplitude or phase field and developing devices with these properties has been a focus of much research into these spatially frequency sensitive metasurfaces. We note, however, that this operation still comes with significant loss of information, specifically the relative sign of gradients within a field as well as more subtly varying phase variations introduced by, for example, the interior features of a sample such as an unstained cell. This can be recovered by introducing a phase bias through off-normal illumination or controlling interference effects using polarization, effectively adding a constant to the OTF. This introduces interference between the background and scattered light producing a pseudo three-dimensional image, similar to that seen in DIC, that contains significantly more information about the sample. A useful concept in characterising optical imaging systems is the numerical aperture (NA). It is defined by the range of angles that can be captured by a lens with

$$\mathrm{NA} = n \sin \theta_{acc}, \tag{6}$$

where θ_{acc} is the maximum acceptance angle of the lens measured relative to normal incidence and n the refractive index of the medium in which the lens is placed. The concept of a numerical aperture is also used in the field of spatial frequency selective meta-optical filters. However, the use of the term in this field is less strictly defined. Here we define the $\mathrm{NA}_{\mathrm{ms}}$ of such a meta-optical filter as half of the the range of normalised spatial frequencies over which the device performs the intended operation, such as high-pass filtering, or exhibiting

a near-linear or parabolic transfer function. With this definition, we obtain

$$\mathrm{NA_{ms}} = n(\sin\theta_{\max} - \sin\theta_{\min})/2, \tag{7}$$

where $\theta_{\max}$ and $\theta_{\min}$ define the maximum and minimum angles of incidence of plane wave components for which the meta-surfaces perform the filtering operation. This definition is, for example, used in Zhou et al.[18] and Wesemann et al.[19]. It is therefore crucial to make a difference between the NA of the meta-optical filter and the $\mathrm{NA_{ms}}$ of the broader imaging system in which the filter is located. Going forward we will only refer to the NA of a metasurface for simplicity since this perspective does not discuss the numerical aperture of imaging systems themselves.

We here divide the various approaches using spatial frequency selective meta-optics into two sections. The first involves metasurfaces where a particular resonance of the unit cell possesses a fundamental sensitivity to the angle of incidence of a plane wave. The second incorporates diffraction gratings and resonant waveguide gratings where the angular response is inherently nonlocal.

3.2.1 Metasurfaces with a phase sensitive unit cell

The resonances of the unit cell of a metasurface can depend on the wavelength, polarization and direction of an incident plane wave. One example includes so-called bound states in the continuum (BICs) that describe confined electromagnetic and other waves that coexist with a continuous spectrum that can permit radiation under appropriate conditions.[126,127] This concept was first introduced in quantum mechanics,[128] but their applications in the form of quasi-BICs in photonic systems has attracted considerable recent attention.[129] Note that the use of this terminology in optics is relatively new and similar physics has previously been described in terms of so-called 'dark' or 'subradiant' modes.[130] Owing to their ability to produce sharp resonances, significant research has focused on applications in sensing,[131–133]

nonlinear effects,[134,135] and in lasing.[136,137] While BICs and subradiant modes are primarily associated with low-loss and high-quality dielectric elements,[129] symmetry-protected BICs have been observed in plasmonic structures.[138,139] Many investigations into BICs introduce a geometric asymmetry to excite quasi- BICs at normal incidence. However, their symmetry in momentum space can also be broken through the use of off-normal incidence. When incorporated into a metasurface, the excitation of BICs manifests as an angle-dependent transmission or reflection and, hence, such devices can be utilized to perform all-optical image processing in the object plane (Fig. 1b).

In metallic nanostructures, the resonance of a metal nanoparticle, often referred to as localized surface plasmon resonance (LSPR), is dominated by the electric dipole moment of the oscillating charge. However, under certain conditions, ensembles of metallic nanoparticle arrangements can be sensitive to phase variations in the incident field and, hence, the angle of incidence.[140–142] This property emerges from the existence of a higher order mode with zero net electric dipole moment that exhibits a symmetry that precludes their excitation with a normally incident plane wave. As with BICs the introduction of a geometric asymmetry leads to the appearance of a quasi-subradiant mode, but, again, when a symmetric plasmonic structure is illuminated with off-normally incident light with a particular polarization, phase shifts across the unit cell are introduced and lead to the excitation of subradiant modes of the unit cell.

Dark modes in plasmonic nanostructures have been used as a platform to convert phase gradient information in weakly absorbing objects into intensity information. The object plane approach to image processing (Fig. 1b) was experimentally demonstrated in reflection with a reflective metasurface consisting of periodic arrays of silver trimer structures that support subradiant modes.[143] The dark mode resonances were excited under linear polarization at oblique angles and an edge enhanced image in reflection was obtained at the resonant wavelength.[144] The optical responses of an array of annular apertures in a perfectly conducting film and arrangements of plasmonic nanorods in a 'dolmen' configuration

were investigated by Roberts *et al.*[145] and it was shown that the angular/spatial frequency sensitivity of the TEM cavity mode of a coaxial aperture or a cross-polarized mode of the plasmonic nanorod ensemble permitted the generation of a dark field image on transmission at the resonant wavelength. Furthermore, a pseudo-3D visualization of the phase object, similar to those obtained through DIC microscopy, is produced when the metasurface is illuminated at an oblique angle.

The dolmen structure was also shown to exhibit an asymmetric optical transfer function across a relatively high numerical aperture (NA) of approximately 0.4 by tuning the orientations of the input polarizer and output analyzer.[146] The device consists of two parallel gold nanorods and a third oriented at 90° to the other pair. The third rod is centered slightly above the two parallel rods. In contrast to structures mentioned previously, if this device is illuminated with linearly polarized light oriented at 45° to the nanorod orientations, while analyzed through a polarizer with its axis parallel to the nanorod pair the OTF of this device is asymmetric about normal incidence, i.e., about zero spatial frequency. Hence, phase visualization, in theory, can be performed at normal incidence. The potential use of this device for image processing was proposed with simulations showing that if a pure phase object is illuminated, with polarizers set as as discussed above, a pseudo-3D phase contrast image should result. Contrast switching is also apparent when the input polarizer is rotated through 90°. The contrast of approximately 10%, however, is low presenting significant challenges to experimental realization.

3.2.2 Non-local metasurfaces

In the previous section, we have shown that phase imaging in the object, image, or other plane can been realized through the use of surfaces whose reflective or transmissive properties are a function of angles of incidence. Other than arrays of metallic nanoparticles, the presence of angle-sensitive transmission and reflection are commonly seen in gratings. In this section, we discuss phase imaging via the object plane approach (Fig. 1b) using these. The distinctions

between the structures discussed here and in the previous section is the mechanism that generates the relevant transfer function.

It should be noted that single optical interfaces, as well stacks of optically thin films, commonly exhibit transmission and reflection properties that enable phase visualisation techniques which fall into this category.[118,147–160] In this perspective, however, we exclusively focus on approaches based on metasurfaces and gratings.

The non-local structures discussed here consist of diffraction and resonant waveguide gratings that do not necessarily exhibit an angular sensitivity in the unit cell. Rather than interacting with the unit cell, gratings modify the spatial frequency content of a field by redirecting plane waves of different frequencies into discrete directions or coupling light into waveguide modes of a high index layer. The first demonstration of non-local image processing of an amplitude object demonstrating edge-enhacement was performed using a thick phase grating as early as 1979.[161] Overvig and Alù point out that the clear delineation between local- and non-local metasurfaces is, however, not necessarily straightforward.[162]

The interaction of light with diffraction gratings, whether on a semi-infinite substrate or on (or part of) a waveguiding layer are well-known to have a strong sensitivity to angle of incidence and there have been a number of demonstrations of image processing applications using this approach. This has included the use of the excitation of Fano resonances to demonstrate the capacity to obtain the second derivative of an input (amplitude) field with a Si grating on a Si waveguiding layer.[14]

In terms of phase contrast imaging, a silver grating supported by a high index TiO_2 waveguiding layer patterning a microscope cover slip was used to image human cancer (HeLa) cells[19] (3a). This structure exhibits a symmetric, near-linear, optical transfer function across a numerical aperture of $\sim$0.06. At normal incidence, this device functions as a high-pass spatial filter, producing edge-enhanced intensity images of both amplitude and phase objects. In the absence of the metasurface, no details of the HeLa cells placed in a petri dish on top of the coverslip, were distinguishable. However, when the cells were on a patterned region

of the coverslip, a pseudo-3D contrast image became apparent on tilting the device by 3°. This small tilt offsets the optical transfer function sufficiently to produce an asymmetric sensitivity to positive and negative angles of incidence. The image produced through the metasurface was shown to be comparable to DIC phase contrast images of the same cells demonstrating the possibility of the application of this technique to miniaturized microscopy systems permitting imaging of unstained biological cells for diagnostic and other uses.

More recently, Ji *et al.*[20] performed phase retrieval using a silicon nitride dielectric resonant waveguide grating (Fig. 3b). Isotropic phase contrast is observed when a phase object (in this case a binary USAF target) is placed in front of the nonlocal metasurface in the imaging system. The result is comparable to the contrast generated by Zernike phase contrast microscopy with a device NA of up to 0.97. Phase contrast images of onion cells, human osteosarcoma cells, and an array of exfoliated hexagonal Boron Nitride (hBN) flakes were also presented, showing the capability of this device to perform phase imaging on objects of various dimensions. Furthermore, quantitative phase retrieval was performed using arrays of silicon nanodisks of different heights as phase objects with the recovered phase profile consistent with those expected with a precision down to 0.02 π.

Phase contrast imaging with a device consisting of an array of plasmonic nanorods in a unit cell supported by a waveguiding layer was also demonstrated by Wesemann *et al.*[21] (Fig. 3d). In this case out-of-phase excitation of dipole modes of orthogonally oriented nanorods was produced using illumination with circularly polarised light, and a further phase shift in the light coupled into the waveguiding layer was introduced by tailoring their spatial separation. This resulted in an asymmetric total transmission through the device about normal incidence which, as discussed above, is required to discriminate between positive and negative gradients within an image. The resulting OTF of this device is inherently asymmetric enabling the creation of pseudo-3D intensity images when illuminated with an optical field containing a phase variation. Due to the chirality of the unit cell geometry, contrast-switching of the phase gradients occurs when the polarization handedness is switched.

In order to use the same device to perform multiple image processing operations, metasurfaces require the ability to change their optical response by external or internal variations or modifying the illumination in some way. Ji *et al.*,[20] for example, highlighted the fact that the imaging response of their resonant waveguide grating could be tuned by changing the wavelength to generate alternative transfer functions, whereas other devices such as that of Wesemann *et al.*[19] were highly sensitive to the polarization of the input field. Zhang *et al.*[163] also embedded multiple optical transfer functions within a reconfigurable metasurface, where the switching between modalities was performed by mechanical straining of a polydimethylsiloxane (PDMS) layer hosting an array of dielectric nanopillars. They demonstrated different imaging modalities at the same wavelength and without changing the polarization including first and second-order differentiation of an image, as well as bright field imaging. This device was applied to obtaining a dark field image of onion cells.

One of the key benefits of the object plane spatial frequency filtering approach is the flexibility to incorporate the device into various locations within an imaging system. Zhou *et al.*[18] used a 2D array of nanopillars exhibiting a nonlocal response to demonstrate edge enhanced amplitude and phase images (Fig. 3c). In addition to demonstrating scalable fabrication of the device, they used a multilayer transfer technique to locate a differentiating nonlocal metasurface directly onto a metalens producing a compact compound optical element. This work highlights some of the key advantages of flat optics in the production of next-generation compact optical systems.

3.3 Other approaches

In the previous section, we discussed phase imaging techniques that involve placing flat optical components at either the Fourier plane, the object plane, or at some other location within a conventional optical imaging system. Nevertheless, metasurfaces have been used in other ways to visualise or determine phase. The methods discussed in this section include apodization or pupil function engineering for phase visualization, the inclusion of multiple

meta-optics, and techniques where metasurfaces assist in obtaining a quantitative phase map of a sample (Fig. 4). Additionally, we also discuss phase visualization through photodetector integration.

Apodization is the process of modifying the lens pupil plane in an optical system to change its point spread function and, hence, the output image. This process is most well-known for being able to suppress the side lobes of diffraction patterns with a suitable mask.[169] A key difference with the research described in the previous two sections is that, firstly, the metasurface is non-uniform and the unit cell varies across the device and, secondly, it is located in proximity to the lens rather than in the Fourier plane. Most notably Kim *et al.*[164] and Zhang *et al.*[170] demonstrated that isotropic edge enhanced images can be obtained of biological cells. The former[164] superimposes a spiral phase profile onto that of a parabolic metalens (Fig. 4a) while the latter[170] achieves simultaneous spiral phase contrast and bright-field imaging within the same field of view (FOV) by incorporating spiral, parabolic, and deflection phases. These papers demonstrate the high degree of integration obtainable with meta-optics permitting broadband imaging of erythrocytes and limewood stem cells respectively. A related demonstration of this approach with the meta-lens and the apodization component placed on opposite sites of a shared substrate is introduced in Fu *et al.*[165] (Fig. 4b). The authors demonstrate the versatility of this approach by engineering the apodisation function for spatial differentiation, denoising, edge detection, and contrast enhancement. Demonstrations of the method for edge detection of onion epidermis cells and DNA molecules highlight its relevance for ultra compact phase imaging systems.

Metasurfaces can also be used to introduce a splitting of the optical field and generate a spatial shear between the beams, permitting the visualization of gradients along one or more directions upon interference. Wang *et al.*[168] introduced what they refer to as metasurface-assisted 'Isotropic Differential Interference Contrast' (i-DIC) microscopy (Fig. 4e). Traditional DIC microscopy visualizes phase gradients along one fixed direction. In contrast, the approach demonstrated by the authors creates a shear in the radial direction, enabling

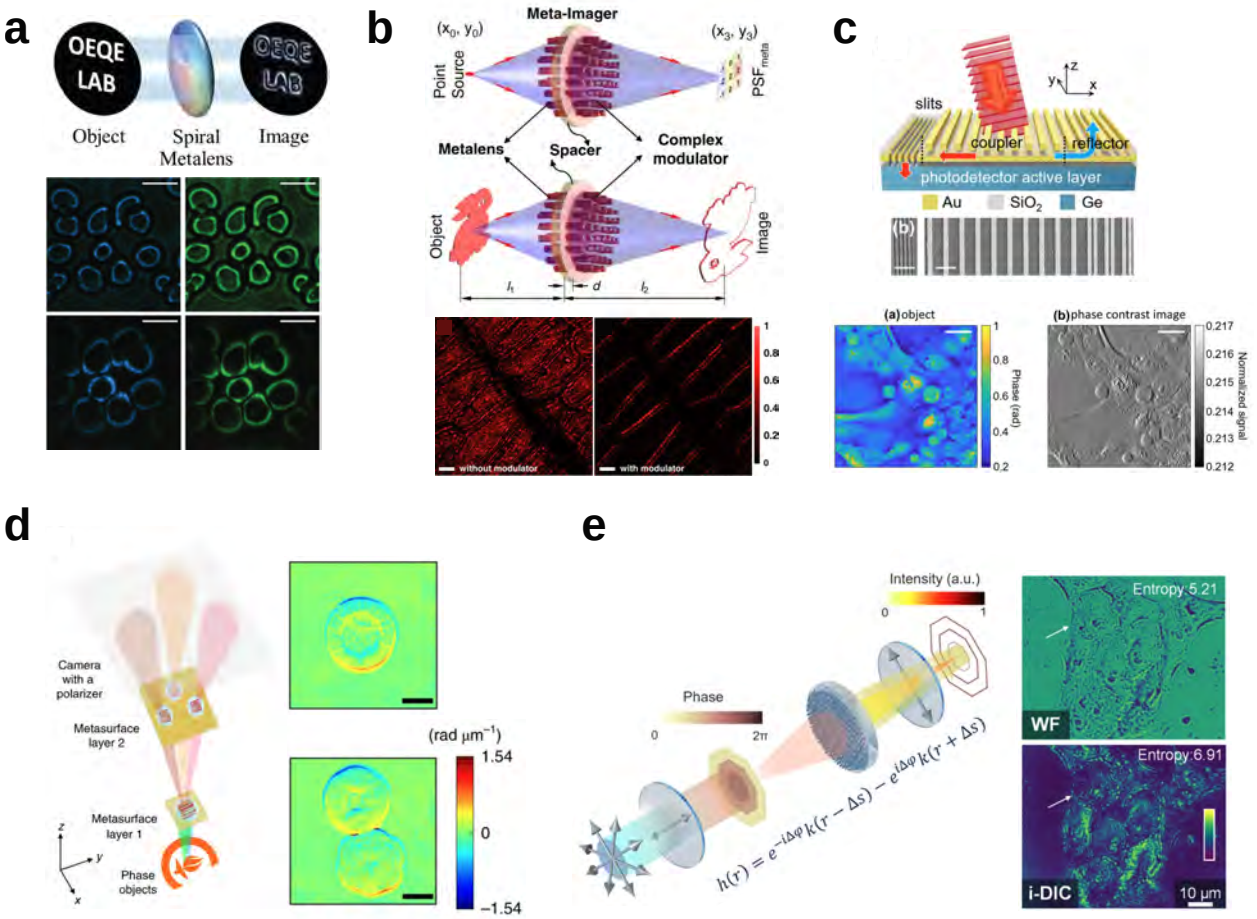

Figure 4: Other methods for metasurface enabled phase-imaging including hybrid analog/digital approaches for quantitative phase-imaging. **a)** Lens apodization with meta optics. Spiral phase profile imposed on parabolic metalens for edge detection (top) and application to phase imaging of erythrocytes (bottom).[164] Copyright 2021 Author(s), licensed under a Creative Commons Attribution (CC BY 4.0) license. **b)** Lens apodization with meta-lens and complex amplitud modulator on opposite sites of the same substrate (top). Detection of edges in unstained onion epidermis cell sample (bottom).[165] Copyright 2022 Author(s), licensed under a Creative Commons Attribution (CC BY-NC-ND 4.0) license. **c)** Meta-optical photodetector for phase imaging (top) and application to quantitative phase contrast imaging of epithelial cells (MCF-10A) (bottom).[166] Copyright 2023 Author(s), licensed under a Creative Commons Attribution (CC BY 4.0) license. **d)** Multiple metasurface approach for polarisation shear and recombination supporting quantitative phase imaging (left). Quantitative phase gradient imaging of sea urchin cells (right). Adapted from ref.[167] with permission from Springer Nature. **e)** i-DIC microscopy: metasurface enabled radial shear and subsequent interference permit isotropic phase gradient visualisation (left). Widefield and phase gradient visualisation of breast cancer cells (right).[168] Copyright 2023 Author(s), licensed under a Creative Commons Attribution (CC BY 4.0) license.

single-shot imaging of isotropic phase gradient images. The performance of this device was demonstrated in real-time tracking of microparticles and phase contrast imaging of breast cancer cells.

There is an emerging interest in using such metasurface enabled methods based on beam shearing and subsequent interference to enable applications requiring quantitative phase imaging (*cf.* section 2.2). For example, Kwon *et al.*[171] utilized two metasurfaces on either side of a substrate acquiring three distinct images incorporating varying phase retardances within a single shot. The first layer captures two images for transverse electric (TE) and transverse magnetic (TM) polarizations at transversely sheared focal points, while the second incorporates three metalenses that produce three sheared images with different phase offsets. The resulting intensity images provide sufficient information to extract the phase. Wu *et al.*[167] introduce an approach utilizing two metasurfaces (Fig. 4d). The first separates incident linearly polarized light into two circularly polarized components propagating in different directions introducing a shear, while the second deflects and recombines the two beams into their initial directions. The retardance image is formed through the interference between the two laterally displaced replicas of the image, where the bias retardation is controlled by the analyzer.

Using a quite different approach, Sardana *et al.*[172] employed a dielectric metasurface acting simultaneously as a metalens and a polarizing beam splitter to produce a single path interferometer. The resulting interference fringes ca be analyzed to obtain QPIs of transparent objects.

Finally, a quite different approach to recovering the phase of an optical wavefield was introduced by Liu *et al.*[166] Fig. (4c). They demonstrate an angle-sensitive, grating-integrated near-infrared photodetector that is capable of performing wavefront sensing with the only other optical component being an imaging lens. The gratings have an asymmetric sensitivity to angle of incidence such that alternating pixels have an equal and an opposite responsivity (Fig. 4c).

4 Current challenges

There are a number of issues that need to be addressed before the full potential of metaoptics in phase imaging applications can be realized. The first is the numerical aperture of the device which determines the range of spatial frequencies that can be manipulated using a particular component.

In the case of metasurfaces incorporated into a $4f$ imaging system as novel spatial filters this is related to the precision and overall size of the device and the optics used. For a metasurface using in the object or image plane, however, this is complex and relates to how well the sensitivity to angle of incidence can be controlled. Many devices demonstrated to date exhibit a relatively low numerical aperture and, although images of microscopic samples have been achieved, are best suited to images of larger objects or integration into an image sensor.[166] There has been worked aimed at extending the numerical aperture of systems. For example, Zhou *et al.*,[18] reported a nonlocal differentiator with an NA of 0.32 and used it to obtained edge-enhanced images of onion cells and Ji *et al.*[20] presented a Zernike phase contrast microscopy inspired nonlocal metasurface with an NA approaching unity. We anticipate that the increasing use of sophisticated optimization routines will permit the creation of a range of devices where an appropriate NA can be selected. Davis *et al.*[146] obtained the one-dimensional transfer function of a dolmen metasurface and, with appropriate inclusion of polarizers, demonstrated an approximately linear transfer function up to an NA of 0.4. This work, however, highlighted another key challenge facing the use of metaoptics for applications in image processing. When a device is used in a $4f$ system as a spatial filter its efficiency will determine the total amount of light transmitted through the system. For devices designed to be used in the object or image plane, on the other hand, the efficiency is related to the usable contrast afforded by the device. Specifically, a certain range of spatial frequencies is mapped to a change in intensity. A device with a high NA may not be suitable for imaging larger objects consisting of only low spatial frequency information since this will correspond to only weak changes in intensity that may be lost in

system noise. Ultimately, the quality with which this information is processed will depend on the noise introduced by the camera. This issue will influence the quality of low spatial frequency information when imaging any objects. Ultimately, it is this noise that will impact the fidelity of the system and its phase sensitivity, not the device itself assuming the device quality is such that background scattering is low. In addition to image artefacts related to the numerical aperture of the metasurfaces, detailed studies on further aberrations emerging from the proposed methods are still to be performed in the majority of cases. This makes evaluating the suitability of a particular method for an application difficult, and we expect progress in this area to be a crucial step towards the adoption of metasurface enabled phase imaging methods.

The scalability of meta-optical devices, particularly metasurfaces, also offers a challenge towards advancing the field. Many devices mentioned in this perspective is commonly fabricated using lithography via electron beam. While this method has been shown to be useful for prototyping and testing devices, creating these devices across a larger area beyond hundreds of square micro-meters is currently expensive and time consuming. Deep UV lithography[173] can be employed to generate nanostructures at a large scale, although the resolution is still limited to about 90 nm. Furthermore, the ongoing developing of nanofabrication methods, such as nano-imprint lithography[174] which includes the roll-to-roll and roll-to-plate techniques,[175,176] and 3D laser writing,[177] offers potential avenues for solving these problems.

Another issue that has received little attention is the role played by spatial coherence. Most devices discussed here assume a high degree of coherence although partial coherence is often preferred in applications in microscopy due to the reduced influence of speckle. Recently, however, theoretical[178] and experimental[179] investigations involving nanophotonic structures and optimized multilayer thin films, respectively, and computational post-processing for incoherent image processing suggest that further advances can be expected.

5 Future opportunities and conclusion

The work reviewed in this perspective highlights the spectrum of emerging meta optical approaches to phase imaging. In the final section of this perspective we outline areas that we believe carry significant potential for future developments.

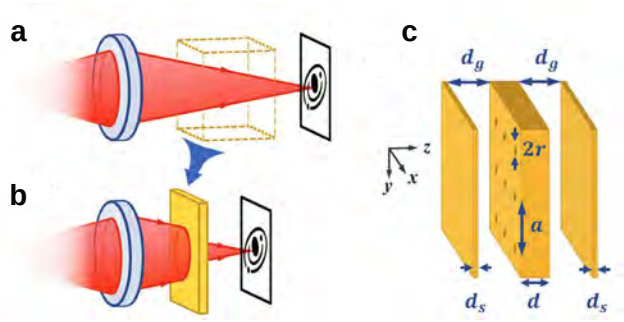

Figure 5: Simulating free-space propagation with nonlocal meta-optical device **(a,b)**. Photonic crystal slab as an example for a device that enables compression of free space to reduce propagation distances in ultra compact optical systems **(c)**. Adapted with permission from ref.[115] , copyright Optical Society of America Publishing Group.

The majority of the demonstrations of meta-optical phase imaging methods to date still require operation in tandem with conventional imaging components such as microscope objectives and polarisers. We envisage compound devices, that integrate several meta-optical components, as a promising path towards real-world ultra compact systems. Existing work in this direction has demonstrated integrating several meta optical components.[18,168] One of the main limiting factors for the miniaturisation of compound imaging optics is the requirement for free space propagation. Recent theoretical work demonstrated that meta-optical devices referred to as 'space plates' carry the potential to simulate free space propagation while reducing the physical distances required.[115] The comparison, for example, is presented in Fig. 5. In the context of compound devices, such space plates could reduce the required spacing between different meta-optical elements. Devices consisting of several metasurfaces or thin-films could also be directly integrated with photodetectors or optical fibers[180,181] opening new avenues for the application of this technology in mobile phones and medical

diagnostic tools.

Opportunities also present for performing 3-D phase retrieval and reconstruction, for example, by employing metasurfaces that can facilitate QPI using tomography techniques.[182–184] In order to perform this technique with the current devices, however, additional mechanisms to rotate the sample would be required or novel designs for reconfigurable metasurfaces.

There is also significant potential in the development of meta-optical filters for phase-imaging that implement useful operations which have received little attention so far. These include for example low-pass filters for noise reduction, and polarisation and wavelength multiplexed filter devices. The design of such filters usually requires non-intuitive designs for which we expect inverse-design strategies as a promising path forward for the next generation of meta-optical imaging components.[185]

Most of the current work on meta-optical phase imaging relies on linear and classical optical effects. Non-linear frequency conversion however plays an important role in conventional imaging approaches. Initial work has demonstrated its potential for meta-optical phase imaging approaches.[27] These approaches could enable phase imaging at infrared wavelengths with either conventional silicon cameras or by eye. Furthermore, translating known principles from quantum imaging into the domain of meta optics could enable integrated quantum phase-imaging.[186] Metasurfaces provide an intriguing platform for quantum processes including the generation of non-classical light and the manipulation and detection of quantum states.[187] We expect quantum effects in metasurfaces to open new avenues in super-resolution imaging, ghost phase-imaging and low-light imaging.[188–191]

While most current meta-optical imaging devices are primarily designed for one operation, their integration into real systems will require a degree of tunability. Initial demonstrations of tunable edge detectors[163,192–194] suggest further exploration of tuning mechanisms for phase-imaging methods including phase change materials, micro electromechanical system (MEMS),[195] liquid crystals[196] and conductive polymers.[197]

One of the most promising future direction for meta-optical phase imaging can be found

at the intersection of nanotechnology and digital computation, in particular artificial intelligence (AI). AI has proven to be of fundamental importance to modern quantitative phase imaging methods.[198] This has enabled software based methods for phase quantification, error correction, contrast enhancement as well as image segmentation, classification and translation operations such as virtual staining. We expect the confluence of these AI approaches and meta-optics to lead to new integrated quantitative phase-imaging methods in the near future. Although this perspective has focused on far-field optical effects, there is also scope for further leveraging nanophotonics and their near-field phase sensitivity for phase recovery in conjunction with computational techniques such as ptychographic coherent diffractive imaging.[96] Meta optical image processing devices also carry potential as hardware accelerators that replace digital computation steps in conventional computational phase imaging methods (c.f. section 2.3) and other machine-vision applications.[23,199,200] Such approaches could support real-time phase imaging and cell identification in high speed applications. Another challenge that could be addressed with the help of AI is the requirement for coherent illumination in most current meta-optical phase imaging methods. This is a common scenario relevant for imaging through scattering media as for example a biological cell in solution. The integration of meta optical components with electronic systems has been used to circumvent this requirement for edge detection filters.[178] We believe machine learning approaches will be central in relaxing spatial coherence requirements in compact phase-imaging methods going forward.[201] Finally, machine learning models are likely to play a key role in metasurface design and optimisation going forward and we expect this to make an important contribution to the field of metasurface enabled phase imaging.[202]

Given that spatial resolution is a critical performance indicator for any imaging method, especially in biology, we anticipate that approaches to super resolution imaging will play a significant role in inspiring future metasurface-assisted phase imaging.[203]

In conclusion, metasurfaces open new avenues for ultra-compact phase imaging methods and we anticipate that the most compelling advances will progress in collaboration with

potential end users. Here we have briefly reviewed existing approaches to phase imaging followed by a comprehensive summary of metasurface-enabled phase imaging methods. We believe that metasurfaces will represent important building blocks for future phase imaging systems and expect significant advances in the field over the coming years.

Acknowledgement

This research was funded by the Australian Government through the Australian Research Council Centre of Excellence grant (CE200100010). S.B.S acknowledges the support of the Ernst & Grace Matthaei Scholarship and the Australian Government Research Training Program Scholarship. N.P. acknowledges the support of a Melbourne Research Scholarship.

Authors' contributions

The manuscript was designed and planned by L.W with assistance from A.R. Section 2 of the manuscript was written by S.B.S, while section 3 was written by N.P with contributions from A.R and L.W. Sections 1, 4 and 5 of the manuscript were written by A.R and L.W with contributions from N.P. All authors provided input on the manuscript.

References

(1) Zou, X.; Lin, R.; Fu, Y.; Gong, G.; Zhou, X.; Wang, S.; Zhu, S.; Wang, Z. Advanced optical imaging based on metasurfaces. *Advanced Optical Materials* **2023**, 2203149.

(2) Lee, D.; Gwak, J.; Badloe, T.; Palomba, S.; Rho, J. Metasurfaces-based imaging and applications: from miniaturized optical components to functional imaging platforms. *Nanoscale Advances* **2020**, *2*, 605–625.

(3) Kamali, S. M.; Arbabi, E.; Arbabi, A.; Faraon, A. A review of dielectric optical metasurfaces for wavefront control. *Nanophotonics* **2018**, *7*, 1041–1068.

(4) Dorrah, A. H.; Rubin, N. A.; Zaidi, A.; Tamagnone, M.; Capasso, F. Metasurface optics for on-demand polarization transformations along the optical path. *Nature Photonics* **2021**, *15*, 287–296.

(5) Wang, S.; Wen, S.; Deng, Z.-L.; Li, X.; Yang, Y. Metasurface-Based Solid Poincaré Sphere Polarizer. *Phys. Rev. Lett.* **2023**, *130*, 123801.

(6) Deng, Y.; Cai, Z.; Ding, Y.; Bozhevolnyi, S. I.; Ding, F. Recent progress in metasurface-enabled optical waveplates. *Nanophotonics* **2022**, *11*, 2219–2244.

(7) Khorasaninejad, M.; Zhu, W.; Crozier, K. Efficient polarization beam splitter pixels based on a dielectric metasurface. *Optica* **2015**, *2*, 376–382.

(8) Zhang, X.; Deng, R.; Yang, F.; Jiang, C.; Xu, S.; Li, M. Metasurface-Based Ultrathin Beam Splitter with Variable Split Angle and Power Distribution. *ACS Photonics* **2018**, *5*, 2997–3002.

(9) Li, J.; Ye, H.; Wu, T.; Liu, Y.; Yu, Z.; Wang, Y.; Sun, Y.; Yu, L. Ultra-broadband large-angle beam splitter based on a homogeneous metasurface at visible wavelengths. *Opt. Express* **2020**, *28*, 32226–32238.

(10) Li, J.; Sun, Y.; Fan, H.; Wang, X.; Ye, H.; Liu, Y. Enabling broadband efficient beam splitting based on ultra-thin reflecting metasurfaces. *Results in Physics* **2023**, *44*, 106181.

(11) Abdelraouf, O. A.; Wang, Z.; Liu, H.; Dong, Z.; Wang, Q.; Ye, M.; Wang, X. R.; Wang, Q. J.; Liu, H. Recent advances in tunable metasurfaces: materials, design, and applications. *ACS nano* **2022**, *16*, 13339–13369.

(12) Wesemann, L.; Davis, T. J.; Roberts, A. Meta-optical and thin film devices for all-optical information processing. *Applied Physics Reviews* **2021**, *8*.

(13) Bykov, D. A.; Doskolovich, L. L.; Morozov, A. A.; Podlipnov, V. V.; Bezus, E. A.; Verma, P.; Soifer, V. A. First-order optical spatial differentiator based on a guided-mode resonant grating. *Optics express* **2018**, *26*, 10997–11006.

(14) Cordaro, A.; Kwon, H.; Sounas, D.; Koenderink, A. F.; Alù, A.; Polman, A. High-Index Dielectric Metasurfaces Performing Mathematical Operations. *Nano Letters* **2019**, *19*, 8418–8423, PMID: 31675241.

(15) Kou, S. S.; Yuan, G.; Wang, Q.; Du, L.; Balaur, E.; Zhang, D.; Tang, D.; Abbey, B.; Yuan, X.-C.; Lin, J. On-chip photonic Fourier transform with surface plasmon polaritons. *Light: Science & Applications* **2016**, *5*, e16034–e16034.

(16) Ahmed, M.; Al-Hadeethi, Y.; Bakry, A.; Dalir, H.; Sorger, V. J. Integrated photonic FFT for photonic tensor operations towards efficient and high-speed neural networks. *Nanophotonics* **2020**, *9*, 4097–4108.

(17) Cordaro, A.; Edwards, B.; Nikkhah, V.; Alù, A.; Engheta, N.; Polman, A. Solving integral equations in free space with inverse-designed ultrathin optical metagratings. *Nature Nanotechnology* **2023**, *18*, 365–372.

(18) Zhou, Y.; Zheng, H.; Kravchenko, I. I.; Valentine, J. Flat optics for image differentiation. *Nature Photonics* **2020**, *14*, 316–323.

(19) Wesemann, L.; Rickett, J.; Song, J.; Lou, J.; Hinde, E.; Davis, T. J.; Roberts, A. Nanophotonics enhanced coverslip for phase imaging in biology. *Light: Science & Applications* **2021**, *10*, 98.

(20) Ji, A.; Song, J.-H.; Li, Q.; Xu, F.; Tsai, C.-T.; Tiberio, R. C.; Cui, B.; Lalanne, P.; Kik, P. G.; Miller, D. A. B.; Brongersma, M. L. Quantitative phase contrast imaging with a nonlocal angle-selective metasurface. *Nature Communications* **2022**, *13*, 7848.

(21) Wesemann, L.; Rickett, J.; Davis, T. J.; Roberts, A. Real-time phase imaging with an asymmetric transfer function metasurface. *ACS Photonics* **2022**, *9*, 1803–1807.

(22) Schroeder, T. Imaging stem-cell-driven regeneration in mammals. *Nature* **2008**, *453*, 345–351.

(23) Zangeneh-Nejad, F.; Sounas, D. L.; Alù, A.; Fleury, R. Analogue computing with metamaterials. *Nature Reviews Materials* **2021**, *6*, 207–225.

(24) Zernike, F. Phase contrast, a new method for the microscopic observation of transparent objects. *Physica* **1942**, *9*, 686–698.

(25) Zernike, F. Phase contrast, a new method for the microscopic observation of transparent objects part II. *Physica* **1942**, *9*, 974–986.

(26) Holzner, C.; Feser, M.; Vogt, S.; Hornberger, B.; Baines, S. B.; Jacobsen, C. Zernike phase contrast in scanning microscopy with X-rays. *Nature Physics* **2010**, *6*, 883–887.

(27) Qiu, X.; Li, F.; Zhang, W.; Zhu, Z.; Chen, L. Spiral phase contrast imaging in nonlinear optics: seeing phase objects using invisible illumination. *Optica* **2018**, *5*, 208–212.

(28) Bernet, S.; Jesacher, A.; Fürhapter, S.; Maurer, C.; Ritsch-Marte, M. Quantitative imaging of complex samples by spiral phase contrast microscopy. *Optics Express* **2006**, *14*, 3792–3805.

(29) Trusiak, M.; Cywińska, M.; Micó, V.; Picazo-Bueno, J. A.; Zuo, C.; Zdańkowski, P.; Patorski, K. Variational Hilbert Quantitative Phase Imaging. *Scientific Reports* **2020**, *10*, 13955.

(30) Arnison, M. R.; Cogswell, C. J.; Smith, N. I.; Fekete, P. W.; Larkin, K. G. Using the Hilbert transform for 3D visualization of differential interference contrast microscope images. *Journal of Microscopy* **2000**, *199*, 79–84.

(31) Lang, W. *Nomarski Differential Interference-Contrast Microscopy*; Carl Zeiss, 1982.

(32) Cui, X.; Lew, M.; Yang, C. Quantitative differential interference contrast microscopy based on structured-aperture interference. *Applied Physics Letters* **2008**, *93*.

(33) Ford, T. N.; Chu, K. K.; Mertz, J. Phase-gradient microscopy in thick tissue with oblique back-illumination. *Nature Methods* **2012**, *9*, 1195–1197.

(34) Hamilton, D. K.; Sheppard, C. J. R.; Wilson, T. Improved imaging of phase gradients in scanning optical microscopy. *Journal of Microscopy* **1984**, *135*, 275–286.

(35) Hoffman, R.; Gross, L. E. O. The modulation contrast microscope. *Nature* **1975**, *254*, 586–588.

(36) Hoffman, R.; Gross, L. Modulation Contrast Microscope. *Applied Optics* **1975**, *14*, 1169–1176.

(37) Molesini, G.; Bertani, D.; Cetica, M. Dark Ground Microscopy With Detuned Interference Filters. *Optical Engineering* **1982**, *21*, 216061.

(38) Macnab, R. M. Examination of bacterial flagellation by dark-field microscopy. *Journal of Clinical Microbiology* **1976**, *4*, 258–265.

(39) Rienitz, J. Schlieren experiment 300 years ago. *Nature* **1975**, *254*, 293–295.

(40) Allen, H. H. Detection of Inhomogeneities in Transparent Plastic Sheet by a Simple Schlieren Technique. *Nature* **1957**, *180*, 50–50.

(41) Zhou, W.-J.; Halpern, A. R.; Seefeld, T. H.; Corn, R. M. Near Infrared Surface Plasmon Resonance Phase Imaging and Nanoparticle-Enhanced Surface Plasmon Resonance Phase Imaging for Ultrasensitive Protein and DNA Biosensing with Oligonucleotide and Aptamer Microarrays. *Analytical Chemistry* **2012**, *84*, 440–445.

(42) Steiner, G. Surface plasmon resonance imaging. *Analytical and Bioanalytical Chemistry* **2004**, *379*, 328–331.

(43) Peterson, A. W.; Halter, M.; Tona, A.; Plant, A. L. High resolution surface plasmon resonance imaging for single cells. *BMC Cell Biology* **2014**, *15*, 35.

(44) Balaur, E.; O'Toole, S.; Spurling, A. J.; Mann, G. B.; Yeo, B.; Harvey, K.; Sadatnajafi, C.; Hanssen, E.; Orian, J.; Nugent, K. A.; others Colorimetric histology using plasmonically active microscope slides. *Nature* **2021**, *598*, 65–71.

(45) Wu, D.; Luo, J.; Huang, G.; Feng, Y.; Feng, X.; Zhang, R.; Shen, Y.; Li, Z. Imaging biological tissue with high-throughput single-pixel compressive holography. *Nature Communications* **2021**, *12*, 4712.

(46) Hu, X.; Zhang, H.; Zhao, Q.; Yu, P.; Li, Y.; Gong, L. Single-pixel phase imaging by Fourier spectrum sampling. *Applied Physics Letters* **2019**, *114*.

(47) Ortolano, G.; Paniate, A.; Boucher, P.; Napoli, C.; Soman, S.; Pereira, S. F.; Ruo-Berchera, I.; Genovese, M. Quantum enhanced non-interferometric quantitative phase imaging. *Light: Science & Applications* **2023**, *12*, 171.

(48) Hodgson, H.; Zhang, Y.; England, D.; Sussman, B. Reconfigurable phase contrast microscopy with correlated photon pairs. *Applied Physics Letters* **2023**, *122*.

(49) Agero, U.; Mesquita, L.; Neves, B.; Gazzinelli, R.; Mesquita, O. Defocusing microscopy. *Microscopy Research and Technique* **2004**, *65*, 159–165.

(50) Paganin, D.; Mayo, S. C.; Gureyev, T. E.; Miller, P. R.; Wilkins, S. W. Simultaneous phase and amplitude extraction from a single defocused image of a homogeneous object. *Journal of Microscopy* **2002**, *206*, 33–40.

(51) Baran, P. et al. High-Resolution X-Ray Phase-Contrast 3-D Imaging of Breast Tissue

Specimens as a Possible Adjunct to Histopathology. *IEEE Transactions on Medical Imaging* **2018**, *37*, 2642–2650.

(52) Pham, H. V.; Bhaduri, B.; Tangella, K.; Best-Popescu, C.; Popescu, G. Real Time Blood Testing Using Quantitative Phase Imaging. *PLOS ONE* **2013**, *8*, e55676.

(53) Holló, C. T.; Mihăltz, K.; Kurucz, M.; Csorba, A.; Kránitz, K.; Kovács, I.; Nagy, Z. Z.; Erdei, G. Objective quantification and spatial mapping of cataract with a Shack-Hartmann wavefront sensor. *Scientific Reports* **2020**, *10*, 12585.

(54) Küppers, M.; Albrecht, D.; Kashkanova, A. D.; Lühr, J.; Sandoghdar, V. Confocal interferometric scattering microscopy reveals 3D nanoscopic structure and dynamics in live cells. *Nature Communications* **2023**, *14*, 1962.

(55) Steelman, Z. A.; Coker, Z. N.; Sedelnikova, A.; Keppler, M. A.; Kiester, A. S.; Troyanova-Wood, M. A.; Ibey, B. L.; Bixler, J. N. Comprehensive single-shot biophysical cytometry using simultaneous quantitative phase imaging and Brillouin spectroscopy. *Scientific Reports* **2022**, *12*, 18285.

(56) Choi, W.; Fang-Yen, C.; Badizadegan, K.; Oh, S.; Lue, N.; Dasari, R. R.; Feld, M. S. Tomographic phase microscopy. *Nature Methods* **2007**, *4*, 717–719.

(57) Shanmugam, P.; Light, A.; Turley, A.; Falaggis, K. Variable shearing holography with applications to phase imaging and metrology. *Light: Advanced Manufacturing* **2022**, *3*, 193.

(58) Khadir, S.; Bon, P.; Vignaud, D.; Galopin, E.; McEvoy, N.; McCloskey, D.; Monneret, S.; Baffou, G. Optical Imaging and Characterization of Graphene and Other 2D Materials Using Quantitative Phase Microscopy. *ACS Photonics* **2017**, *4*, 3130–3139.

(59) Hogenboom, D. O.; DiMarzio, C. A.; Gaudette, T. J.; Devaney, A. J.; Lindberg, S. C. Three-dimensional images generated by quadrature interferometry. *Optics Letters* **1998**, *23*, 783–785.

(60) Wang, Z.; Millet, L.; Mir, M.; Ding, H.; Unarunotai, S.; Rogers, J.; Gillette, M. U.; Popescu, G. Spatial light interference microscopy (SLIM). *Optics Express* **2011**, *19*, 1016–1026.

(61) He, Y. R.; He, S.; Kandel, M. E.; Lee, Y. J.; Hu, C.; Sobh, N.; Anastasio, M. A.; Popescu, G. Cell Cycle Stage Classification Using Phase Imaging with Computational Specificity. *ACS Photonics* **2022**, *9*, 1264–1273.

(62) Kandel, M. E.; He, Y. R.; Lee, Y. J.; Chen, T. H.-Y.; Sullivan, K. M.; Aydin, O.; Saif, M. T. A.; Kong, H.; Sobh, N.; Popescu, G. Phase imaging with computational specificity (PICS) for measuring dry mass changes in sub-cellular compartments. *Nature Communications* **2020**, *11*, 6256.

(63) Nguyen, T. H.; Kandel, M. E.; Rubessa, M.; Wheeler, M. B.; Popescu, G. Gradient light interference microscopy for 3D imaging of unlabeled specimens. *Nature Communications* **2017**, *8*, 210.

(64) Kandel, M. E.; Hu, C.; Naseri Kouzehgarani, G.; Min, E.; Sullivan, K. M.; Kong, H.; Li, J. M.; Robson, D. N.; Gillette, M. U.; Best-Popescu, C.; Popescu, G. Epi-illumination gradient light interference microscopy for imaging opaque structures. *Nature Communications* **2019**, *10*, 4691.

(65) Singh Mehta, D.; Srivastava, V. Quantitative phase imaging of human red blood cells using phase-shifting white light interference microscopy with colour fringe analysis. *Applied Physics Letters* **2012**, *101*.

(66) Iwai, H.; Fang-Yen, C.; Popescu, G.; Wax, A.; Badizadegan, K.; Dasari, R. R.;

Feld, M. S. Quantitative phase imaging using actively stabilized phase-shifting low-coherence interferometry. *Optics Letters* **2004**, *29*, 2399–2401.

(67) Shibata, N.; Findlay, S. D.; Kohno, Y.; Sawada, H.; Kondo, Y.; Ikuhara, Y. Differential phase-contrast microscopy at atomic resolution. *Nature Physics* **2012**, *8*, 611–615.

(68) Polanco, E. R.; Moustafa, T. E.; Butterfield, A.; Scherer, S. D.; Cortes-Sanchez, E.; Bodily, T.; Spike, B. T.; Welm, B. E.; Bernard, P. S.; Zangle, T. A. Multiparametric quantitative phase imaging for real-time, single cell, drug screening in breast cancer. *Communications Biology* **2022**, *5*, 794.

(69) Fan, Y.; Sun, J.; Chen, Q.; Pan, X.; Trusiak, M.; Zuo, C. Single-shot isotropic quantitative phase microscopy based on color-multiplexed differential phase contrast. *APL Photonics* **2019**, *4*.

(70) Tamamitsu, M.; Toda, K.; Shimada, H.; Honda, T.; Takarada, M.; Okabe, K.; Nagashima, Y.; Horisaki, R.; Ideguchi, T. Label-free biochemical quantitative phase imaging with mid-infrared photothermal effect. *Optica* **2020**, *7*, 359–366.

(71) Jo, Y.; Park, S.; Jung, J.; Yoon, J.; Joo, H.; Kim, M.-h.; Kang, S.-J.; Choi, M. C.; Lee, S. Y.; Park, Y. Holographic deep learning for rapid optical screening of anthrax spores. *Science Advances* **2017**, *3*, e1700606.

(72) Monemhaghdoust, Z.; Montfort, F.; Emery, Y.; Depeursinge, C.; Moser, C. Off-axis digital holographic camera for quantitative phase microscopy. *Biomedical Optics Express* **2014**, *5*, 1721–1730.

(73) Min, J.; Yao, B.; Trendafilova, V.; Ketelhut, S.; Kastl, L.; Greve, B.; Kemper, B. Quantitative phase imaging of cells in a flow cytometry arrangement utilizing Michelson interferometer-based off-axis digital holographic microscopy. *Journal of Biophotonics* **2019**, *12*, e201900085.

(74) Popescu, G.; Ikeda, T.; Dasari, R. R.; Feld, M. S. Diffraction phase microscopy for quantifying cell structure and dynamics. *Optics Letters* **2006**, *31*, 775–777.

(75) Wang, F.; Liu, L.; Yu, P.; Liu, Z.; Yu, H.; Wang, Y.; Li, W. J. Three-Dimensional Super-Resolution Morphology by Near-Field Assisted White-Light Interferometry. *Scientific Reports* **2016**, *6*, 24703.

(76) Mann, P.; Singh, V.; Tayal, S.; Thapa, P.; Mehta, D. S. White light phase shifting interferometric microscopy with whole slide imaging for quantitative analysis of biological samples. *Journal of Biophotonics* **2022**, *15*, e202100386.

(77) Park, Y.; Choi, W.; Yaqoob, Z.; Dasari, R.; Badizadegan, K.; Feld, M. S. Speckle-field digital holographic microscopy. *Optics Express* **2009**, *17*, 12285–12292.

(78) Wang, C.; Fu, Q.; Dun, X.; Heidrich, W. Quantitative Phase and Intensity Microscopy Using Snapshot White Light Wavefront Sensing. *Scientific Reports* **2019**, *9*, 13795.

(79) Rinehart, M. T.; Jaedicke, V.; Wax, A. Quantitative phase microscopy with off-axis optical coherence tomography. *Optics Letters* **2014**, *39*, 1996–1999.

(80) Sticker, M.; Hitzenberger, C. K.; Leitgeb, R.; Fercher, A. F. Quantitative differential phase measurement and imaging in transparent and turbid media by optical coherence tomography. *Optics Letters* **2001**, *26*, 518–520.

(81) Kim, T.; Zhou, R.; Mir, M.; Babacan, S. D.; Carney, P. S.; Goddard, L. L.; Popescu, G. White-light diffraction tomography of unlabelled live cells. *Nature Photonics* **2014**, *8*, 256–263.

(82) Zhao, J.; Matlock, A.; Zhu, H.; Song, Z.; Zhu, J.; Wang, B.; Chen, F.; Zhan, Y.; Chen, Z.; Xu, Y.; Lin, X.; Tian, L.; Cheng, J.-X. Bond-selective intensity diffraction tomography. *Nature Communications* **2022**, *13*, 7767.

(83) Kim, G. et al. Rapid species identification of pathogenic bacteria from a minute quantity exploiting three-dimensional quantitative phase imaging and artificial neural network. *Light: Science & Applications* **2022**, *11*, 190.

(84) Bon, P.; Monneret, S.; Wattellier, B. Noniterative boundary-artifact-free wavefront reconstruction from its derivatives. *Applied Optics* **2012**, *51*, 5698–5704.

(85) Gerchberg, R. W.; Saxton, W. O. A practical algorithm for the determination of phase from image and diffraction plane pictures. *Optik* **1972**, *35*, 237–246.

(86) Fienup, J. R. Phase retrieval algorithms: a comparison. *Applied Optics* **1982**, *21*, 2758–2769.

(87) Morgan, K. S.; Paganin, D. M. Applying the Fokker–Planck equation to grating-based x-ray phase and dark-field imaging. *Scientific Reports* **2019**, *9*, 17465.

(88) Leatham, T. A.; Paganin, D. M.; Morgan, K. S. X-Ray Dark-Field and Phase Retrieval Without Optics, via the Fokker–Planck Equation. *IEEE Transactions on Medical Imaging* **2023**, *42*, 1681–1695.

(89) Streibl, N. Phase imaging by the transport equation of intensity. *Optics Communications* **1984**, *49*, 6–10.

(90) Zuo, C.; Li, J.; Sun, J.; Fan, Y.; Zhang, J.; Lu, L.; Zhang, R.; Wang, B.; Huang, L.; Chen, Q. Transport of intensity equation: a tutorial. *Optics and Lasers in Engineering* **2020**, *135*, 106187.

(91) Li, J.; Zhou, N.; Sun, J.; Zhou, S.; Bai, Z.; Lu, L.; Chen, Q.; Zuo, C. Transport of intensity diffraction tomography with non-interferometric synthetic aperture for three-dimensional label-free microscopy. *Light: Science & Applications* **2022**, *11*, 154.

(92) Engay, E.; Huo, D.; Malureanu, R.; Bunea, A.-I.; Lavrinenko, A. Polarization-dependent all-dielectric metasurface for single-shot quantitative phase imaging. *Nano Letters* **2021**, *21*, 3820–3826.

(93) Jiang, S.; Song, P.; Wang, T.; Yang, L.; Wang, R.; Guo, C.; Feng, B.; Maiden, A.; Zheng, G. Spatial- and Fourier-domain ptychography for high-throughput bio-imaging. *Nature Protocols* **2023**, *18*, 2051–2083.

(94) Faulkner, H. M. L.; Rodenburg, J. M. Movable Aperture Lensless Transmission Microscopy: A Novel Phase Retrieval Algorithm. *Physical Review Letters* **2004**, *93*, 023903.

(95) Zheng, G.; Horstmeyer, R.; Yang, C. Wide-field, high-resolution Fourier ptychographic microscopy. *Nature Photonics* **2013**, *7*, 739–745.

(96) Balaur, E.; Cadenazzi, G. A.; Anthony, N.; Spurling, A.; Hanssen, E.; Orian, J.; Nugent, K. A.; Parker, B. S.; Abbey, B. Plasmon-induced enhancement of ptychographic phase microscopy via sub-surface nanoaperture arrays. *Nature Photonics* **2021**, *15*, 222–229.

(97) Wang, F.; Bian, Y.; Wang, H.; Lyu, M.; Pedrini, G.; Osten, W.; Barbastathis, G.; Situ, G. Phase imaging with an untrained neural network. *Light: Science & Applications* **2020**, *9*, 77.

(98) Huang, L.; Liu, T.; Yang, X.; Luo, Y.; Rivenson, Y.; Ozcan, A. Holographic Image Reconstruction with Phase Recovery and Autofocusing Using Recurrent Neural Networks. *ACS Photonics* **2021**, *8*, 1763–1774.

(99) Ayyappan, V.; Chang, A.; Zhang, C.; Paidi, S. K.; Bordett, R.; Liang, T.; Barman, I.; Pandey, R. Identification and Staging of B-Cell Acute Lymphoblastic Leukemia Using Quantitative Phase Imaging and Machine Learning. *ACS Sensors* **2020**, *5*, 3281–3289.

(100) Nguyen, T. H.; Sridharan, S.; Macias, V.; Kajdacsy-Balla, A.; Melamed, J.; Do, M.; Popescu, G. Automatic Gleason grading of prostate cancer using quantitative phase imaging and machine learning. *Journal of Biomedical Optics* **2017**, *22*, 036015.

(101) Chen, H.-T.; Taylor, A. J.; Yu, N. A review of metasurfaces: physics and applications. *Reports on Progress in Physics* **2016**, *79*, 076401.

(102) Li, J.; Li, J.; Zhou, S.; Yi, F. Metasurface photodetectors. *Micromachines* **2021**, *12*, 1584.

(103) Piyasena, M. E.; Graves, S. W. The intersection of flow cytometry with microfluidics and microfabrication. *Lab on a Chip* **2014**, *14*, 1044–1059.

(104) Zhou, P.; He, H.; Ma, H.; Wang, S.; Hu, S. A review of optical imaging technologies for microfluidics. *Micromachines* **2022**, *13*, 274.

(105) Liddle, J. D.; Holt, A. P.; Jason, S. J.; O'Donnell, K. A.; Stevens, E. J. Space science with CubeSats and nanosatellites. *Nature Astronomy* **2020**, *4*, 1026–1030.

(106) Beckers, J. M. Adaptive optics for astronomy: principles, performance, and applications. *Annual review of astronomy and astrophysics* **1993**, *31*, 13–62.

(107) O'Neill, E. Spatial filtering in optics. *IRE Transactions on Information Theory* **1956**, *2*, 56–65.

(108) Elias, P. Optics and communication theory. *Journal of the Optical Society of America* **1953**, *43*, 229–232.

(109) Goodman, J. W. *Introduction to Fourier optics*; Roberts and Company publishers, 2005.

(110) Pors, A.; Nielsen, M. G.; Bozhevolnyi, S. I. Analog Computing Using Reflective Plasmonic Metasurfaces. *Nano Letters* **2015**, *15*, 791–797, PMID: 25521830.

(111) Huo, P.; Zhang, C.; Zhu, W.; Liu, M.; Zhang, S.; Zhang, S.; Chen, L.; Lezec, H. J.; Agrawal, A.; Lu, Y.; others Photonic spin-multiplexing metasurface for switchable spiral phase contrast imaging. *Nano Letters* **2020**, *20*, 2791–2798.

(112) Zhou, J.; Qian, H.; Zhao, J.; Tang, M.; Wu, Q.; Lei, M.; Luo, H.; Wen, S.; Chen, S.; Liu, Z. Two-dimensional optical spatial differentiation and high-contrast imaging. *National science review* **2021**, *8*, nwaa176.

(113) Zhou, J.; Wu, Q.; Zhao, J.; Posner, C.; Lei, M.; Chen, G.; Zhang, J.; Liu, Z. Fourier optical spin splitting microscopy. *Physical review letters* **2022**, *129*, 020801.

(114) Overvig, A. C.; Shrestha, S.; Malek, S. C.; Lu, M.; Stein, A.; Zheng, C.; Yu, N. Dielectric metasurfaces for complete and independent control of the optical amplitude and phase. *Light: Science & Applications* **2019**, *8*, 92.

(115) Guo, C.; Wang, H.; Fan, S. Squeeze free space with nonlocal flat optics. *Optica* **2020**, *7*, 1133–1138.

(116) Pancharatnam, S.; Pancharatnam, S. Generalized theory of interference, and its applications. *Resonance* **2013**, *18*, 387–389.

(117) Berry, M. V. Quantal phase factors accompanying adiabatic changes. *Proceedings of the Royal Society of London. A. Mathematical and Physical Sciences* **1984**, *392*, 45–57.

(118) Bliokh, K. Y. Geometrodynamics of polarized light: Berry phase and spin Hall effect in a gradient-index medium. *Journal of Optics A: Pure and Applied Optics* **2009**, *11*, 094009.

(119) Bomzon, Z.; Biener, G.; Kleiner, V.; Hasman, E. Space-variant Pancharatnam–Berry phase optical elements with computer-generated subwavelength gratings. *Opt. Lett.* **2002**, *27*, 1141–1143.

(120) Xu, D.; Yang, H.; Xu, W.; Zhang, W.; Zeng, K.; Luo, H. Inverse design of Pancharatnam–Berry phase metasurfaces for all-optical image edge detection. *Applied Physics Letters* **2022**, *120*.

(121) Shou, Y.; Wang, Y.; Miao, L.; Chen, S.; Luo, H. Realization of all-optical higher-order spatial differentiators based on cascaded operations. *Optics Letters* **2022**, *47*, 5981–5984.

(122) Wang, Y.; Yang, Q.; He, S.; Wang, R.; Luo, H. Computing metasurfaces enabled broad-band vectorial differential interference contrast microscopy. *ACS Photonics* **2022**,

(123) Zhou, J.; Qian, H.; Chen, C.-F.; Zhao, J.; Li, G.; Wu, Q.; Luo, H.; Wen, S.; Liu, Z. Optical edge detection based on high-efficiency dielectric metasurface. *Proceedings of the National Academy of Sciences* **2019**, *116*, 11137–11140.

(124) Yu, N.; Genevet, P.; Kats, M. A.; Aieta, F.; Tetienne, J.-P.; Capasso, F.; Gaburro, Z. Light Propagation with Phase Discontinuities: Generalized Laws of Reflection and Refraction. *Science* **2011**, *334*, 333–337.

(125) Li, Z.; Shang, S.; Liao, W.; Tang, F.; Wu, J.; Zeng, T.; Kong, B.; Ye, X.; Jiang, X.; Yang, L.; others Optical edge-enhanced imaging based on dielectric metasurfaces. *Optical Materials* **2023**, *143*, 114206.

(126) Hsu, C. W.; Zhen, B.; Stone, A. D.; Joannopoulos, J. D.; Soljačić, M. Bound states in the continuum. *Nature Reviews Materials* **2016**, *1*, 16048.

(127) Kang, M.; Liu, T.; Chan, C. T.; Xiao, M. Applications of bound states in the continuum in photonics. *Nature Reviews Physics* **2023**, *5*, 659–678.

(128) Von Neumann, J.; Wigner, E. On some peculiar discrete eigenvalues. *Phys. Z* **1929**, *30*, 465–467.

(129) Koshelev, K.; Bogdanov, A.; Kivshar, Y. Meta-optics and bound states in the continuum. *Science Bulletin* **2019**, *64*, 836–842, SPECIAL TOPIC: Electromagnetic Metasurfaces: from Concept to Applications.

(130) Chu, M.-W.; Myroshnychenko, V.; Chen, C. H.; Deng, J.-P.; Mou, C.-Y.; García de Abajo, F. J. Probing Bright and Dark Surface-Plasmon Modes in Individual and Coupled Noble Metal Nanoparticles Using an Electron Beam. *Nano Letters* **2009**, *9*, 399–404, PMID: 19063614.

(131) Yanik, A. A.; Cetin, A. E.; Huang, M.; Artar, A.; Mousavi, S. H.; Khanikaev, A.; Connor, J. H.; Shvets, G.; Altug, H. Seeing protein monolayers with naked eye through plasmonic Fano resonances. *Proceedings of the National Academy of Sciences* **2011**, *108*, 11784–11789.

(132) Romano, S.; Zito, G.; Torino, S.; Calafiore, G.; Penzo, E.; Coppola, G.; Cabrini, S.; Rendina, I.; Mocella, V. Label-free sensing of ultralow-weight molecules with all-dielectric metasurfaces supporting bound states in the continuum. *Photonics Research* **2018**, *6*, 726–733.

(133) Yesilkoy, F.; Arvelo, E. R.; Jahani, Y.; Liu, M.; Tittl, A.; Cevher, V.; Kivshar, Y.; Altug, H. Ultrasensitive hyperspectral imaging and biodetection enabled by dielectric metasurfaces. *Nature Photonics* **2019**, *13*, 390–396.

(134) Koshelev, K.; Tang, Y.; Li, K.; Choi, D.-Y.; Li, G.; Kivshar, Y. Nonlinear metasurfaces governed by bound states in the continuum. *Acs Photonics* **2019**, *6*, 1639–1644.

(135) Liu, Z.; Xu, Y.; Lin, Y.; Xiang, J.; Feng, T.; Cao, Q.; Li, J.; Lan, S.; Liu, J. High-Q quasibound states in the continuum for nonlinear metasurfaces. *Physical review letters* **2019**, *123*, 253901.

(136) Meier, M.; Mekis, A.; Dodabalapur, A.; Timko, A.; Slusher, R.; Joannopoulos, J.;

Nalamasu, O. Laser action from two-dimensional distributed feedback in photonic crystals. *Applied Physics Letters* **1999**, *74*, 7–9.

(137) Hwang, M.-S.; Kim, H.-R.; Jeong, K.-Y.; Park, H.-G.; Kivshar, Y. Novel non-plasmonic nanolasers empowered by topology and interference effects. *Nanophotonics* **2021**, *10*, 3599–3611.

(138) Aigner, A.; Tittl, A.; Wang, J.; Weber, T.; Kivshar, Y.; Maier, S. A.; Ren, H. Plasmonic bound states in the continuum to tailor light-matter coupling. *Science Advances* **2022**, *8*, eadd4816.

(139) Liang, Y.; Koshelev, K.; Zhang, F.; Lin, H.; Lin, S.; Wu, J.; Jia, B.; Kivshar, Y. Bound states in the continuum in anisotropic plasmonic metasurfaces. *Nano Letters* **2020**, *20*.

(140) Roberts, A. Beam transmission through hole arrays. *Opt. Express* **2010**, *18*, 2528–2533.

(141) Gómez, D. E.; Teo, Z. Q.; Altissimo, M.; Davis, T. J.; Earl, S.; Roberts, A. The Dark Side of Plasmonics. *Nano Letters* **2013**, *13*, 3722–3728, PMID: 23802620.

(142) Roberts, A.; Davis, T. J.; Gomez, D. E. Dark mode metasurfaces: sensing optical phase difference with subradiant modes and Fano resonances. *JOSA B* **2017**, *34*, D95–D100.

(143) Wesemann, L.; Achmari, P.; Singh, K.; Panchenko, E.; James, T. D.; Gómez, D. E.; Davis, T. J.; Roberts, A. Metasurfaces, dark modes, and high NA illumination. *OSA Continuum* **2018**, *1*, 727–735.

(144) Wesemann, L.; Panchenko, E.; Singh, K.; Gomez, D. E.; Davis, T. J.; Roberts, A. Plasmonic metasurfaces for optical information processing. SPIE Micro + Nano Materials, Devices, and Applications 2019. 2019; p 112010F.

(145) Roberts, A.; Gómez, D. E.; Davis, T. J. Optical image processing with metasurface dark modes. *J. Opt. Soc. Am. A* **2018**, *35*, 1575–1584.

(146) Davis, T.; Eftekhari, F.; Gómez, D.; Roberts, A. Metasurfaces with asymmetric optical transfer functions for optical signal processing. *Physical review letters* **2019**, *123*, 013901.

(147) Youssefi, A.; Zangeneh-Nejad, F.; Abdollahramezani, S.; Khavasi, A. Analog computing by Brewster effect. *Optics letters* **2016**, *41*, 3467–3470.

(148) Zhu, T.; Lou, Y.; Zhou, Y.; Zhang, J.; Huang, J.; Li, Y.; Luo, H.; Wen, S.; Zhu, S.; Gong, Q.; others Generalized spatial differentiation from the spin hall effect of light and its application in image processing of edge detection. *Physical Review Applied* **2019**, *11*, 034043.

(149) Zhu, T.; Huang, J.; Ruan, Z. Optical phase mining by adjustable spatial differentiator. *Advanced Photonics* **2020**, *2*, 016001–016001.

(150) Xu, D.; He, S.; Zhou, J.; Chen, S.; Wen, S.; Luo, H. Goos–Hänchen effect enabled optical differential operation and image edge detection. *Applied Physics Letters* **2020**, *116*.

(151) Zhu, T.; Guo, C.; Huang, J.; Wang, H.; Orenstein, M.; Ruan, Z.; Fan, S. Topological optical differentiator. *Nature communications* **2021**, *12*, 680.

(152) Song, B.; Wen, S.-C.; Shu, W. Topological differential microscopy based on the spin–orbit interaction of light in a natural crystal. *ACS Photonics* **2022**, *9*, 3987–3994.

(153) He, S.; Wang, R.; Xu, W.; Luo, Z.; Luo, H. Visualization of transparent particles based on optical spatial differentiation. *Optics Letters* **2022**, *47*, 5754–5757.

(154) Wang, R.; He, S.; Luo, H. Photonic spin-Hall differential microscopy. *Physical Review Applied* **2022**, *18*, 044016.

(155) Wesemann, L.; Panchenko, E.; Singh, K.; Della Gaspera, E.; Gómez, D. E.; Davis, T. J.; Roberts, A. Selective near-perfect absorbing mirror as a spatial frequency filter for optical image processing. *APL Photonics* **2019**, *4*.

(156) Vohnsen, B.; Valente, D. Surface-plasmon-based wavefront sensing. *Optica* **2015**, *2*, 1024–1027.

(157) Zhu, T.; Zhou, Y.; Lou, Y.; Ye, H.; Qiu, M.; Ruan, Z.; Fan, S. Plasmonic computing of spatial differentiation. *Nature communications* **2017**, *8*, 15391.

(158) Sulejman, S. B.; Priscilla, N.; Wesemann, L.; Lee, W. S. L.; Lou, J.; Hinde, E.; Davis, T. J.; Roberts, A. Thin film notch filters as platforms for biological image processing. *Scientific Reports* **2023**, *13*, 4494.

(159) Jin, C.; Yang, Y. Transmissive nonlocal multilayer thin film optical filter for image differentiation. *Nanophotonics* **2021**, *10*, 3519–3525.

(160) Xue, W.; Miller, O. D. High-NA optical edge detection via optimized multilayer films. *Journal of Optics* **2021**, *23*, 125004.

(161) Case, S. K. Fourier processing in the object plane. *Opt. Lett.* **1979**, *4*, 286–288.

(162) Overvig, A.; Alù, A. Diffractive nonlocal metasurfaces. *Laser & Photonics Reviews* **2022**, *16*, 2100633.

(163) Zhang, X.; Zhou, Y.; Zheng, H.; Linares, A. E.; Ugwu, F. C.; Li, D.; Sun, H.-B.; Bai, B.; Valentine, J. G. Reconfigurable Metasurface for Image Processing. *Nano Letters* **2021**, *21*, 8715–8722, PMID: 34643401.

(164) Kim, Y.; Lee, G.-Y.; Sung, J.; Jang, J.; Lee, B. Spiral metalens for phase contrast imaging. *Advanced Functional Materials* **2022**, *32*, 2106050.

(165) Fu, W.; Zhao, D.; Li, Z.; Liu, S.; Tian, C.; Huang, K. Ultracompact meta-imagers for arbitrary all-optical convolution. *Light: Science & Applications* **2022**, *11*, 62.

(166) Liu, J.; Wang, H.; Li, Y.; Tian, L.; Paiella, R. Asymmetric metasurface photodetectors for single-shot quantitative phase imaging. *arXiv preprint arXiv:2306.06267* **2023**,

(167) Wu, Q.; Zhou, J.; Chen, X.; Zhao, J.; Lei, M.; Chen, G.; Lo, Y.-H.; Liu, Z. Single-shot quantitative amplitude and phase imaging based on a pair of all-dielectric metasurfaces. *Optica* **2023**, *10*, 619–625.

(168) Wang, X.; Wang, H.; Wang, J.; Liu, X.; Hao, H.; Tan, Y. S.; Zhang, Y.; Zhang, H.; Ding, X.; Zhao, W.; others Single-shot isotropic differential interference contrast microscopy. *Nature Communications* **2023**, *14*, 2063.

(169) Slepian, D. Analytic solution of two apodization problems. *JOSA* **1965**, *55*, 1110–1115.

(170) Zhang, Y.; Lin, P.; Huo, P.; Liu, M.; Ren, Y.; Zhang, S.; Zhou, Q.; Wang, Y.; Lu, Y.-q.; Xu, T. Dielectric Metasurface for Synchronously Spiral Phase Contrast and Bright-Field Imaging. *Nano Letters* **2023**, *23*, 2991–2997.

(171) Kwon, H.; Arbabi, E.; Kamali, S. M.; Faraji-Dana, M.; Faraon, A. Single-shot quantitative phase gradient microscopy using a system of multifunctional metasurfaces. *Nature Photonics* **2020**, *14*, 109–114.

(172) Sardana, J.; Devinder, S.; Zhu, W.; Agrawal, A.; Joseph, J. Dielectric Metasurface Enabled Compact, Single-Shot Digital Holography for Quantitative Phase Imaging. *Nano Letters* **2023**,

(173) Srituravanich, W.; Fang, N.; Sun, C.; Luo, Q.; Zhang, X. Plasmonic nanolithography. *Nano letters* **2004**, *4*, 1085–1088.

(174) Wu, D.; S Rajput, N.; Luo, X. Nanoimprint lithography-the past, the present and the future. *Current Nanoscience* **2016**, *12*, 712–724.

(175) Kooy, N.; Mohamed, K.; Pin, L. T.; Guan, O. S. A review of roll-to-roll nanoimprint lithography. *Nanoscale research letters* **2014**, *9*, 1–13.

(176) Ahn, S. H.; Guo, L. J. Large-area roll-to-roll and roll-to-plate nanoimprint lithography: a step toward high-throughput application of continuous nanoimprinting. *ACS nano* **2009**, *3*, 2304–2310.

(177) Zhang, Y.-L.; Chen, Q.-D.; Xia, H.; Sun, H.-B. Designable 3D nanofabrication by femtosecond laser direct writing. *Nano Today* **2010**, *5*, 435–448.

(178) Wang, H.; Guo, C.; Zhao, Z.; Fan, S. Compact incoherent image differentiation with nanophotonic structures. *Acs Photonics* **2020**, *7*, 338–343.

(179) Zhang, X.; Bai, B.; Sun, H.-B.; Jin, G.; Valentine, J. Incoherent Optoelectronic Differentiation Based on Optimized Multilayer Films. *Laser & Photonics Reviews* **2022**, *16*, 2200038.

(180) Li, J.; Thiele, S.; Quirk, B. C.; Kirk, R. W.; Verjans, J. W.; Akers, E.; Bursill, C. A.; Nicholls, S. J.; Herkommer, A. M.; Giessen, H.; others Ultrathin monolithic 3D printed optical coherence tomography endoscopy for preclinical and clinical use. *Light: Science & Applications* **2020**, *9*, 124.

(181) Plidschun, M.; Ren, H.; Kim, J.; Förster, R.; Maier, S. A.; Schmidt, M. A. Ultrahigh numerical aperture meta-fibre for flexible optical trapping. *Light: Science & Applications* **2021**, *10*, 57.

(182) Hugonnet, H.; Han, H.; Park, W.; Park, Y. Improving specificity and axial spatial resolution of refractive index imaging by exploiting uncorrelated subcellular dynamics. *ACS Photonics* **2023**, *11*, 257–266.

(183) Pirone, D.; Sirico, D.; Miccio, L.; Bianco, V.; Mugnano, M.; del Giudice, D.; Pasquinelli, G.; Valente, S.; Lemma, S.; Iommarini, L.; others 3D imaging lipidometry in single cell by in-flow holographic tomography. *Opto Electronic Adv* **2023**, *6*, 220048–220041.

(184) Pirone, D.; Bianco, V.; Miccio, L.; Memmolo, P.; Psaltis, D.; Ferraro, P. Beyond fluorescence: advances in computational label-free full specificity in 3D quantitative phase microscopy. *Current Opinion in Biotechnology* **2024**, *85*, 103054.

(185) Li, Z.; Pestourie, R.; Lin, Z.; Johnson, S. G.; Capasso, F. Empowering metasurfaces with inverse design: principles and applications. *ACS Photonics* **2022**, *9*, 2178–2192.

(186) Gilaberte Basset, M.; Setzpfandt, F.; Steinlechner, F.; Beckert, E.; Pertsch, T.; Gräfe, M. Perspectives for applications of quantum imaging. *Laser & Photonics Reviews* **2019**, *13*, 1900097.

(187) Solntsev, A. S.; Agarwal, G. S.; Kivshar, Y. S. Metasurfaces for quantum photonics. *Nature Photonics* **2021**, *15*, 327–336.

(188) Zanforlin, U.; Lupo, C.; Connolly, P. W.; Kok, P.; Buller, G. S.; Huang, Z. Optical quantum super-resolution imaging and hypothesis testing. *Nature Communications* **2022**, *13*, 5373.

(189) Vega, A.; Pertsch, T.; Setzpfandt, F.; Sukhorukov, A. A. Metasurface-assisted quantum ghost discrimination of polarization objects. *Physical Review Applied* **2021**, *16*, 064032.

(190) Zhou, J.; Liu, S.; Qian, H.; Li, Y.; Luo, H.; Wen, S.; Zhou, Z.; Guo, G.; Shi, B.; Liu, Z. Metasurface enabled quantum edge detection. *Science advances* **2020**, *6*, eabc4385.

(191) Sephton, B.; Nape, I.; Moodley, C.; Francis, J.; Forbes, A. Revealing the embedded phase in single-pixel quantum ghost imaging. *Optica* **2023**, *10*, 286–291.

(192) Xiao, T.; Yang, H.; Yang, Q.; Xu, D.; Wang, R.; Chen, S.; Luo, H. Realization of tunable edge-enhanced images based on computing metasurfaces. *Optics Letters* **2022**, *47*, 925–928.

(193) Khodasevych, I.; Wesemann, L.; Roberts, A.; Iacopi, F. Tunable nonlocal metasurfaces based on graphene for analogue optical computation. *Optical Materials Express* **2023**, *13*, 1475–1487.

(194) Cotrufo, M.; Sulejman, S. B.; Wesemann, L.; Rahman, M. A.; Bhaskaran, M.; Roberts, A.; Alù, A. Reconfigurable Image Processing Metasurfaces with Phase-Change Materials. *arXiv preprint arXiv:2311.13109* **2023**,

(195) Arbabi, E.; Arbabi, A.; Kamali, S. M.; Horie, Y.; Faraji-Dana, M.; Faraon, A. MEMS-tunable dielectric metasurface lens. *Nature communications* **2018**, *9*, 812.

(196) Bosch, M.; Shcherbakov, M. R.; Won, K.; Lee, H.-S.; Kim, Y.; Shvets, G. Electrically actuated varifocal lens based on liquid-crystal-embedded dielectric metasurfaces. *Nano Letters* **2021**, *21*, 3849–3856.

(197) Karst, J.; Floess, M.; Ubl, M.; Dingler, C.; Malacrida, C.; Steinle, T.; Ludwigs, S.; Hentschel, M.; Giessen, H. Electrically switchable metallic polymer nanoantennas. *Science* **2021**, *374*, 612–616.

(198) Park, J.; Bai, B.; Ryu, D.; Liu, T.; Lee, C.; Luo, Y.; Lee, M. J.; Huang, L.; Shin, J.; Zhang, Y.; others Artificial intelligence-enabled quantitative phase imaging methods for life sciences. *Nature Methods* **2023**, *20*, 1645–1660.

(199) Zheng, H.; Liu, Q.; Kravchenko, I. I.; Zhang, X.; Huo, Y.; Valentine, J. G. Multichannel meta-imagers for accelerating machine vision. *Nature Nanotechnology* **2024**, 1–8.

(200) Wang, Z.; Hu, B.; Liu, J.; Wang, G.; Liu, W.; Xiong, C.; Huang, J.; Liu, J.; Zhang, Y. 4f-Less Terahertz Optical Pattern Recognition Enabled by Complex Amplitude Modulating Metasurface Through Laser Direct Writing. *Advanced Optical Materials* **2023**, 2300575.

(201) Lin, H.; Huang, C.; He, Z.; Zeng, J.; Chen, F.; Yu, C.; Li, Y.; Zhang, Y.; Chen, H.; Pu, J. Phase Imaging through Scattering Media Using Incoherent Light Source. Photonics. 2023; p 792.

(202) Qiu, T.; Shi, X.; Wang, J.; Li, Y.; Qu, S.; Cheng, Q.; Cui, T.; Sui, S. Deep learning: a rapid and efficient route to automatic metasurface design. *Advanced Science* **2019**, *6*, 1900128.

(203) Astratov, V. N.; Sahel, Y. B.; Eldar, Y. C.; Huang, L.; Ozcan, A.; Zheludev, N.; Zhao, J.; Burns, Z.; Liu, Z.; Narimanov, E.; others Roadmap on Label-Free Super-Resolution Imaging. *Laser & Photonics Reviews* **2023**, *17*, 2200029.